

**Establishment of a Standardised *in vitro* Assay of Human Monocyte-derived
Macrophages to Investigate the Immunomodulatory Potential of Adipose
Tissue-derived Mesenchymal Stromal Cells**



AALBORG UNIVERSITY
DENMARK

Cardiology
Stem Cell
Centre

Master thesis
Stine Banggaard Hansen

Aalborg University, Medicine with Industrial Specialisation, Biomedicine
9 and 10th semester, Autumn 2020 - Spring 2021

Titelblad

Titel: Etablering af et Standardiseret *in vitro* Assay for Humane Monocyt-deriverede Makrofager til at Undersøge det Immunmodulatoriske Potentiale af Fedtvævs-deriverede Mesenkymale Stromale Celler

Institution:
Aalborg Universitet

Studieretning:
Medicin med Industriel Specialisering,
Biomedicin

Semester:
9-10. Semester

Projektperiode:
Efterår 2020 - Forår 2021

Projektgruppe:
Gruppe 9027

Studerende, studienr.:
Stine Bangsgaard Hansen
20164195

Intern vejleder:
Trine Fink

Ekstern vejleder:
Morten Juhl
Bjarke Follin

Antal Sider:
61

Anslag: 66.883,
Svarende til cirka 41 normalsider

Antal Bilag:
3

Resumé

Makrofager er vigtige immunceller med adskillige funktioner, fra inducering af inflammation til fremmelse af vævsreparation. Det er afspejlet i deres høje plasticitet og fagocytotiske kapacitet. I dette studie genererede vi pro- og anti-inflammatoriske monocyt-deriverede makrofager (M1 and M2) via polariserende cytokiner (henholdsvis GM-CSF og M-CSF). Ud fra disse umodne fænotyper, blev tre distinkte modne makrofager genereret via aktiverende stimuli: mM1(LPS+IFN γ), M2a (IL-4) and M2c (IL-10) makrofager.

Vi demonstrerede, at den udviklede *in vitro* protokol til differentiering og aktivering af makrofager var anvendelig og brugbar i et assay til at vurdere de immunmodulatoriske egenskaber af Fedtvævs-deriverede Mesenkymale Stromale Celler (AT-MSc) på makrofager. Ved at co-kulturerer AT-MSc med makrofager under aktivering, faldt ekspresionen af modne markører på modne M1 makrofager, og deres evne til at inducere proliferation af allogene lymfocytter var signifikant hæmmet. Herudover demonstrerede vi, at AT-MSc havde evnen til at booste de anti-inflammatoriske M2a og M2c fænotyper.

Skiftet fra modne M1 makrofager til en mindre pro-inflammatorisk fænotype, induceret af AT-MSc, kan være gunstig til ophævelse af inflammationen observeret i adskillige sygdomme, og fremmelsen af M2-fænotyper kan formodentligt hjælpe med at genskabe normal funktion.

Title Page

Title:

Establishment of a Standardised *in vitro* Assay of Human Monocyte-derived Macrophages to Investigate the Immunomodulatory Potential of Adipose Tissue-derived Mesenchymal Stromal Cells

Institution:

Aalborg University

Field of Study:

Medicine with Industrial Specialisation,
Biomedicine

Semester:

9/10th Semester

Project Period:

Autumn 2020- Spring 2021

Project Group:

Group 9027

Student, study number:

Stine Bangsgaard Hansen
20164195

Intern supervisor:

Trine Fink

Extern supervisor:

Morten Juhl
Bjarke Follin

Number of Pages:

61

Character Count: 66,883

Approximately 41 pages

Number of Appendices:

3

Abstract

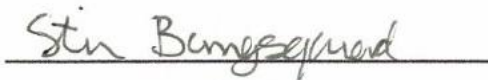
Macrophages are important immune cells with diverse functions, from inducing inflammation to encouraging tissue repair. This is reflected in their high plasticity and phagocytotic capacity. In this study, we generated pro- and anti-inflammatory monocyte-derived macrophages (M1 and M2) by polarising cytokines (GM-CSF and M-CSF, respectively). From these immature phenotypes, three distinct mature macrophages were generated by activating stimuli: mM1(LPS+IFN γ), M2a (IL-4) and M2c (IL-10) macrophages.

We demonstrated that the developed *in vitro* protocol for differentiation and activation of macrophages was applicable and useful in an assay to assess the immunomodulatory properties of Adipose Tissue-derived Mesenchymal Stromal Cells (AT-MSC) on macrophages. By co-culturing AT-MSC with macrophages during activation, the expression of maturation markers decreased on mature M1 macrophages and their ability to induce proliferation of allogeneic lymphocytes was significantly suppressed. Additionally, we demonstrated that AT-MSC had the ability to boost the anti-inflammatory M2a and M2c phenotypes.

The shift of mature M1 macrophages to a less pro-inflammatory phenotype, induced by AT-MSC, can be favorable to resolution of the inflammation observed in numerous diseases, and the promotion of M2-phenotypes may help restore normal function.

Preface

This thesis is conducted by Stine Bangsgaard Hansen as the final accomplishment of the Master's degree, Medicine with Industrial Specialisation (Biomedicine) at School of Medicine and Health, Aalborg University, in external collaboration with Cardiology Stem Cell Center, Rigshospitalet. The project constitutes 60 ECTS points and is supervised by internal supervisor Associate Professor Trine Fink, Aalborg University, as well as the external supervisors Ph.D. Morten Juhl and Ph.D. and Post Doc fellow Bjarke Follin, Cardiology Stem Cell Center, Rigshospitalet.



Stine Bangsgaard Hansen - 20164195

Copenhagen - 27th of May 2021

Acknowledgements

Thanks to Cardiology Stem Cell Centre and all the colleagues for professional and moral support. You admit the very foundation of this thesis. A special thanks goes to Morten Juhl and Bjarke Follin for your dedication and passionated supervision. There are no words to describe how thankful I am for what you have been given us this year.

Thank you, Camilla Holm Pedersen, for many hours in the laboratory, for professional discussions and for being a good friend. The past year would not have been the same without you. I am sure that you are facing a bright future.

Thanks to my mom and dad, Dorrit and Torben Hansen, you have always been there, believed and supported me the very best you could, thank you! Lastly, thanks my two Jacobs (brother and boyfriend) for technical support in Overleaf and for believing in me in times of despair.

Contents

1	Introduction	1
2	Methods and Materials	4
2.1	Isolation of PBMC and Sorting of Monocytes	4
2.2	Monocyte-Derived Macrophages	5
2.2.1	Activation of Macrophages	6
2.3	Co-culture of AT-MSC and Macrophages	7
2.3.1	Expansion of AT-MSC	7
2.3.2	Juxtacrine and Paracrine Signalling	8
2.4	Harvesting of Macrophages for Analysis	8
2.5	Flow Cytometry	8
2.6	ELISA	10
2.7	Phagocytosis Assay	11
2.8	Mixed Lymphocyte Reaction Assay	12
2.8.1	Flow Cytometry for Mixed Lymphocyte Reaction Assay	13
2.9	Data analysis and Figures	15
3	Results	16
3.1	Cytokine Titration	16
3.1.1	M1 Macrophages: Titration of GM-CSF	16
3.1.2	M2 Macrophages: Titration of M-CSF	16
3.2	Cell Seeding Density	18
3.3	Titration of Activating Stimuli	19
3.3.1	Maturation of M1 macrophages	20

CONTENTS

3.3.2	Maturation of M2a macrophages	26
3.3.3	Maturation of M2c macrophages	26
3.4	Morphological Characteristics and Expression of Markers	29
3.5	AT-MSC ratio	31
3.6	Phagocytosis	35
3.6.1	Bead Concentration and Exposure Time	35
3.7	Co-culture with AT-MSC and Macrophages	37
3.7.1	Effect of AT-MSC on marker expression on M1 macrophages	37
3.7.2	Effect of AT-MSC on marker expression on M2a macrophages	39
3.7.3	Effect of AT-MSC on marker expression on M2c macrophages	40
3.7.4	Mixed Lymphocyte Reaction	42
3.7.5	AT-MSC Impact on the Phagocytotic Properties of Macrophages	43
4	Discussion	46
5	Appendix	59
5.1	Monocytes	59
5.2	Activation of M1 macrophages	59
5.3	Activation of M2c macrophages	60
5.4	Dendritic Cells	61

Abbreviations

AT-MSC	Adipose Tissue-derived Mesenchymal Stromal Cells
BM	Bone Marrow
CSFE	Carboxyfluorescein succinimidyl ester
DAPI	4',6-Diamidino-2-Phenylindole, Dilactate
DC	Dendritic Cells
DI	Division Index
Dil/P	Fraction Diluted
DMSO	Dimethyl sulfoxide
EDTA	Ethylenediaminetetraacetic acid
ELISA	Enzyme-linked Immunosorbent Assay
FACS	Flow Cytometry Staining Buffer
FBS	Fetal Bovine Serum
FVS780	Fixable Viability Stain 780
GM-CSF	Granulocyte-Macrophage Colony-Stimulating Factor
hPL	Human Platelet Lysate
IFN	Interferon
IL	Interleukin
ISCT	International Society for Cellular Therapy
LPS	Lipopolysaccharide
M-CSF	Macrophage Colony-Stimulating Factor
MACS	Magnetic-activated Cell Sorting
MEM	Minimum Essential Medium
MFI	Median Fluorescence Intensity
MLR	Mixed Lymphocyte Reaction
MSC	Mesenchymal Stromal Cells
PBS	Phosphate Buffered Saline
PF	Precursor Frequency
PMBC	Peripheral Blood Mononuclear Cell
PS	Phosphatidylserine
RI	Replication Index
RT	Room Temperature
SE	Standard Error
TLR	Toll-like Receptor
TNF	Tumor Necrosis Factor

1 Introduction

In 1991 Caplan introduced the term *Mesenchymal Stem Cell* [1] based on previous studies [2] such as Tavassoli and Crosby in 1968 [3] and Friedenstein and colleagues in 1987 [4]. Friedenstein et al. showed that cells derived from Bone Marrow (BM) were adherent to plastic and capable of forming colonies. They suggested that these cells, or at least some of them, might act as osteogenic stem cells [4]. Studies of Mesenchymal Stem Cells lead to the paradigm that damaged tissue of mesenchymal origin could be repaired by engraftment and/or differentiation of these cells [1, 5]. However, a paradigm shift have occurred which involves the Mesenchymal Stem Cell ability to generate their own microenvironment [6] and thereby enhance repairment of the damaged tissue [5].

The term Mesenchymal Stem cell have been widely used in research leading to more than 71,000 results when searching for *Mesenchymal Stem cell* at PubMed [7] (figure 1.1). However, the term is inappropriate due to the fact that the unfractionated plastic-adherent cells, derived from BM or other sources, were heterogeneous with different properties, and only a small subset of this population might meet the criteria of stem cells. Therefore, International Society for Cellular Therapy (ISCT) proposed the term multipotent Mesenchymal Stromal Cells (MSC) to be more correct [8–10]. Hence, the term MSC will be used to describe this population throughout this study.

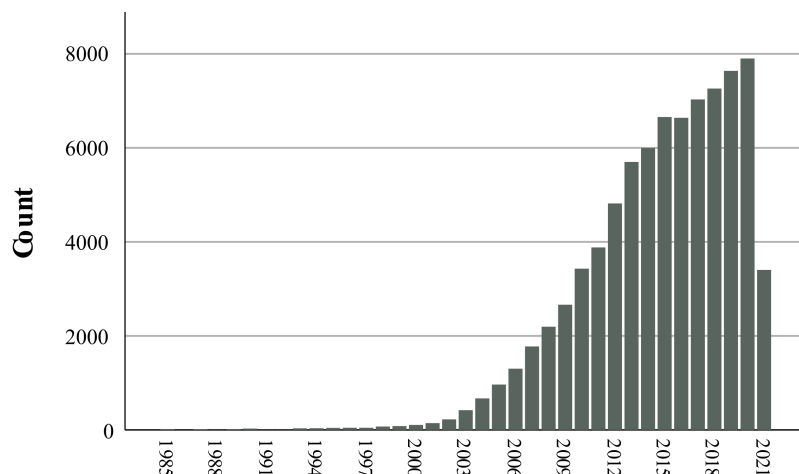


Figure 1.1: Number of results by years when searching *Mesenchymal Stem cell* at Pubmed

MSC can be harvested from several tissues such as BM, placenta and adipose tissue, among others [4, 11, 12], with different pros and cons regarding availability, yield and cell culture expansions [13, 14]. This study will primarily focus on Adipose Tissue-derived Mesenchymal Stromal Cells (AT-MSC). However, independently of the source for MSC, they are characterised by the same minimal

criteria proposed by ISCT [10]. Additionally, several studies have demonstrated that MSC have the ability to induce less pro-inflammatory phenotypes and suppress proliferation of immune cells of the innate and adaptive including Dendritic Cells (DC), T-cells and macrophages, among others [15–17]. As mentioned, MSC can be harvested from different tissues but in this study, we will focus on Adipose Tissue-derived Mesenchymal Stromal Cells (AT-MSC) and their immunomodulatory properties on macrophages.

In 1882 macrophages were discovered by Metchnikoff as phagocytes, which means "*Eating Cells*". He discovered that these cells did not only phagocytise for feeding themselves or other cells but also for defending against invaders [18]. For several decades it was thought that macrophages were derived from monocytes [19] which was only partly correct [20, 21].

In general, monocytes can be differentiated by environmental stimuli into two types of macrophages: pro-inflammatory and anti-inflammatory, also known as M1 and M2 macrophages, respectively [22]. In 1992 it was demonstrated that M2 macrophages could polarise into an *alternative macrophage* also known as M2a [23], activated by Interleukin (IL)-4 and/or IL-13 [23–25]. The following years two additional subtypes of M2 macrophages were discovered, known as M2b and M2c macrophages [26, 27]. Activating stimuli for M2b macrophages includes immunocomplexes, Toll-like Receptor (TLR) ligand or IL-1R [26], while M2c can be generated by IL-10 and/or glucocorticoids [25, 26]. Even though the different subtypes have distinct specialised properties, they have common features such as phagocytotic capacity and display high plasticity [26, 28, 29]. This study will primarily focus on immature M1 and M2 as well as mature M1, M2a and M2c macrophages. Immature M1 and M2 macrophages are characterised as CD14⁺, CD68⁺ and HLA-DR⁺ [28, 30, 31], while the mature M1 phenotype is characterised as CD38⁺, CD86⁺ and HLA-DR⁺, among others [24, 32] and secretion of inflammatory cytokines secretion of Tumor Necrosis Factor (TNF)- α and IL-12 [33]. The M2a macrophage is characterised as CD14⁻ and CD206⁺ [34], whereas the M2c is characterised as CD14⁺ CD163⁺ [34, 35].

It is reported by several studies that MSC have the ability to induce polarisation from M1 into M2 macrophages *in vitro* and *in vivo* by immunomodulation [11, 17, 36, 37]. Barminko et al. suggested that M1 macrophages co-cultured with MSC switch to M2 macrophages characterised as the increased expression of CD206 [36]. This polarisation can be favorable in treatment of inflammatory diseases such as Crohn's disease and chronic wounds, eventually, leading to resolution of the inflammation

[37, 38]. Prior to assessment of the immunomodulatory properties of AT-MSC on the subtypes of macrophages, it is necessary to establish a standardised assay *in vitro*. To our knowledge there is no common well-defined protocol for differentiation and activation of monocyte-derived macrophages *in vitro*. However, there are several studies and recommendations for differentiation of monocytes into macrophages [22, 39, 40]. Therefore, the aim of this thesis is to develop a standardised *in vitro* assay of human monocyte-derived macrophages to investigate the immunomodulatory potential of AT-MSC.

2 Methods and Materials

Several factors have been optimised in order to establish a standardised *in vitro* macrophage protocol for investigations of the immunomodulatory properties of AT-MS. The optimised factors include cytokine titration, cell seeding density, titration of activating stimuli, AT-MS ratio and phagocytosis which is briefly mentioned in the following section and will be further elaborated in the chapter of results (3 Results). The methods used to determine optimal conditions revolved around flow cytometry for measurements of phenotypical marker expression (described in section 2.5), Enzyme-linked Immunosorbent Assay (ELISA) for measurements of cytokine secretion (described in section 2.6) and cell count to determine the viability of cells.

2.1 Isolation of PMBC and Sorting of Monocytes

Monocytes were isolated from fresh buffy coats (Department of Clinical Immunology, Rigshospitalet, Denmark) containing Peripheral Blood Mononuclear Cell (PMBC)s, donated by healthy, anonymised and consenting donors as illustrated in figure 2.1. The buffy coat was diluted in Phosphate Buffered Saline (PBS) to a ratio of 1:3.6 in T75 flask (Thermo Fisher). LeucoSep tubes (Greiner-Bio-One) were centrifuged at 800·g for 30 seconds at Room Temperature (RT) (Hettich Zentrifugen, Rotina 380) with Lymphoprep density gradient (Alere Technologies AS). Subsequently, the diluted buffy coat was gently added to the LeucoSep tubes, and centrifuged at 800·g for 15 minutes at RT to isolate PMBC in the interphase. The harvested PMBC were washed four times with PBS and filtered through a 100 μ m cell strainer (Falcon) before the final centrifugation of PMBC (if not otherwise stated, all centrifugations were performed at 300·g for 5 minutes at RT and supernatant was discarded). Pellet was resuspended in degassed Magnetic-activated Cell Sorting (MACS) buffer, consisting of PBS, 0.5 % Fetal Bovine Serum (FBS) and 2mM Ethylenediaminetetraacetic acid (EDTA). Subsequently, cells were counted on Nucleocounter (NC-100 Chemometec). Cell concentration was adjusted to 1×10^8 cells/ml. CD14⁺ monocytes were positively selected by using magnetic CD14 microbeads and LS columns (Miltenyi Biotec), the instructions from the manufacturer was followed, except the amount of CD14 beads. For every 1×10^8 PMBC, 50 μ l CD14 MicroBeads were added to the cell suspension ($\frac{1}{4}$ of manufacturer's recommendation, previously optimised by CSCC). Isolated CD14⁺ monocytes were counted, washed once by centrifugation and the cell concentration was adjusted to 10^6 cells/ml in medium consisting of RPMI1640 with L-Glutamine (Sigma Aldrich or Gibco), supplemented with

100 units/ml penicillin and 100 ug/ml streptomycin (Gibco) and 10% heat inactivated FBS, henceforth referred to as medium.

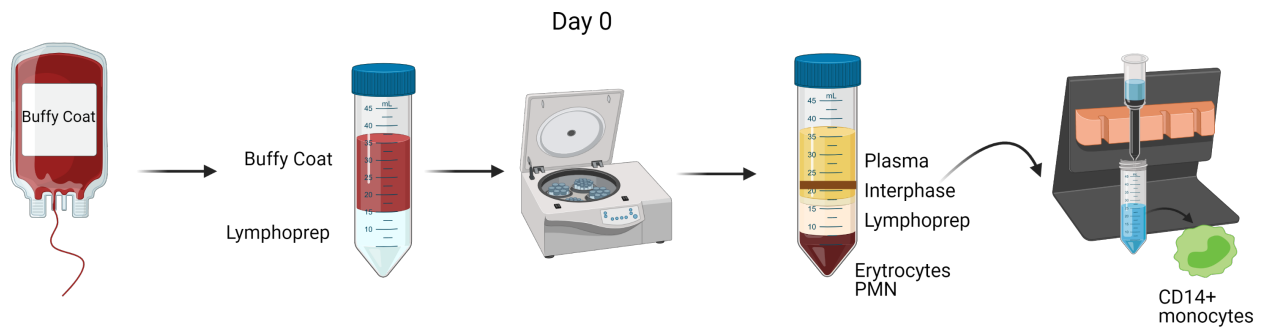


Figure 2.1: Illustration of the procedure for isolation of CD14⁺ monocytes. Initially, PMBC, in the interphase, were isolated from buffy coats by density gradient centrifugation. CD14⁺ monocytes were positively isolated from the heterogeneous cell population, PMBC, by labeling with CD14 beads and magnetic-activated cell sorting. PMN: Polymorphonuclear leukocyte

2.2 Monocyte-Derived Macrophages

5×10^5 CD14⁺ monocytes were seeded per well in untreated 12-well plate (Thermo Fisher Scientific). CD14⁺ monocytes were differentiated into M1 and M2 macrophages by addition of Granulocyte-Macrophage Colony-Stimulating Factor (GM-CSF) (10 ng/ml) and Macrophage Colony-Stimulating Factor (M-CSF) (75 ng/ml) (PeproTech) to the medium, respectively, and incubated at 37°C, 5% CO₂ (HERA cell 150). The optimal concentrations were determined by titrations, as will be addressed later in section 3.1. The polarisation medium was changed every third day. After 7 days of cultivation, immature M1 and M2 macrophages had been generated, illustrated in figure 2.2.

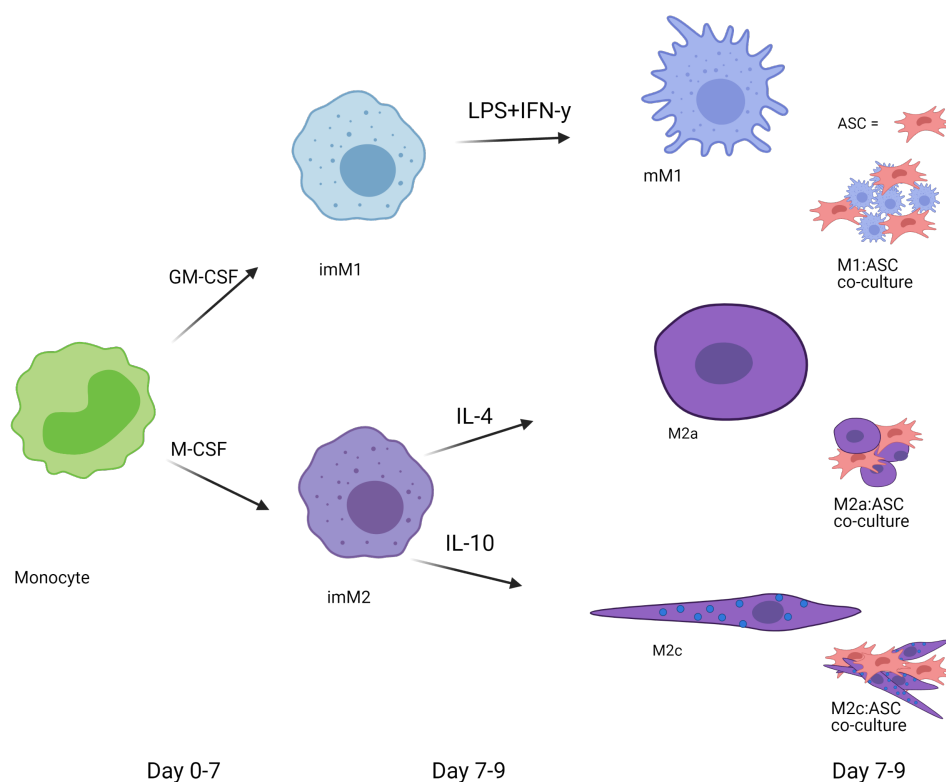


Figure 2.2: Note: ASC is an abbreviation for AT-MSC. Illustration of the experimental cultivation of macrophages. Initially, CD14⁺ monocytes were differentiated into immature M1 and M2 macrophages, by the addition of polarisation cytokines, GM-CSF and M-CSF, respectively. After 7 days of differentiation, the macrophages were either co-cultured with AT-MSC directly or indirectly and activated with different stimuli to generate three distinct mature phenotypes. M1 was activated with LPS in combination with IFN- γ and M2 were either activated with IL-4 or IL-10 to generate M2a and M2c, respectively.

2.2.1 Activation of Macrophages

At day 7, immature macrophages were harvested and reseeded for activation. The plates were centrifuged and supernatant was discarded. 1x TrypLE (Gibco) was added and plates were incubated for 20 minutes at 37°C and 5% CO₂. Cells were collected and TrypLE was inactivated by addition of medium. Wells were washed with PBS which was pooled with the harvested cell suspension, and cells were subsequently centrifuged. Pellet was resuspended in medium followed by cell counting. Cell concentration was adjusted to 3.5×10^5 cells/ml and cells were reseeded for activation. M1 macrophages were activated by polarisation medium supplemented with 500 ng/ml Lipopolysaccharide (LPS) (Sigma) and 5 ng/ml Interferon (IFN)- γ (PeproTech). M2 macrophages were activated with 20 ng/ml IL-4 or 40 ng/ml IL-10 (PeproTech) to generate M2a and M2c, respectively, hence-

forth referred to as activating medium. Optimal seeding density was determined experimentally and activating stimuli were determined by titrations, as presented in section 3.2 and 3.3, respectively. The cells were activated for two days. The maturation of the macrophages is illustrated in figure 2.2. Morphological changes of the different phenotypes were observed by microscopy (EVOS, Life technologies).

2.3 Co-culture of AT-MSC and Macrophages

AT-MSC were included in experimental setups with macrophages, either in juxtacrine or paracrine conditions, to investigate their immunomodulatory properties.

2.3.1 Expansion of AT-MSC

AT-MSC were isolated from lipoaspirate donated by healthy volunteers as described in Haack-Sørensen et al. [12]. In brief, the stromal vascular fraction was expanded in a bioreactor (Quantum system, Terumo BCT) in growth medium consisting of α -MEM, 100 units/ml penicillin and 100 ug/ml streptomycin (Gibco) and 5% hPL (Sexton Biotechnologies), henceforth referred to as AT-MSC medium. AT-MSC were passaged once more in the bioreactor, a total of two passages (P0 and P1). For long term storage, the AT-MSC were cryopreserved after P1 in cryogenic vials (Thermo Fisher Scientific).

For additional expansion of the single donor included in this study, the AT-MSC were thawed in a 37°C water bath until approximately 10% of the cryomedium was left frozen. Subsequently, AT-MSC were diluted in prewarmed AT-MSC medium, centrifuged and resuspended in AT-MSC medium for cell counting on Nucleocounter (NC-100 Chemometec). 5×10^5 AT-MSC were seeded per T175 flask in AT-MSC medium. Medium was changed once before passaging, which occurred when AT-MSC reached a confluency of approximately 90%. For the passaging, AT-MSC medium was discarded and the cells were washed once with PBS. AT-MSC were detached from the flask by incubation of 1x TrypLE (Gibco) for 10 minutes in 37°C and 5% CO₂ (HERA cell 150). Cell suspension was collected and the flask was washed few times with AT-MSC medium. Cells were centrifuged and 5×10^5 AT-MSC were reseeded in each T175 flask. 3 days after reseeded the AT-MSC were harvested as described above. After the final centrifugation, pellet was resuspended in cryomedium, consisting of 10% DMSO in FBS. 1×10^6 AT-MSC were aliquoted into cryogenic vials (Thermo Fisher Scientific) and frozen in CoolCell Containers (Corning) overnight in -80°C for controlled freezing, before long

term storage in liquid nitrogen.

Before use in each setup, the AT-MSC were thawed in waterbath at 37°C for four minutes. AT-MSC in cryomedium was diluted in medium followed by centrifugation. AT-MSC were resuspended in medium and counted.

2.3.2 Juxtacrine and Paracrine Signalling

Co-cultures of immature M1 and M2 macrophages with AT-MSC were established at a ratio of 1:5 (AT-MSC: Macrophage, corresponding to 7×10^4 AT-MSC), in untreated 12-well plates at day 7. The optimal cell concentration of AT-MSC was experimentally determined and is elaborated in section 3.5.

For paracrine signalling, ASC were seeded in hanging inserts with a pore size of $3\mu\text{m}$ (Thermo Fisher Scientific), hanging at the lowest position of the transwell carrier plate. Cells in both types of co-cultures were either activated with M1, M2a or M2c activating medium. Mature and immature macrophages of each phenotype were generated as control by the addition of activating or polarisation medium, respectively. The cells were activated or maintained as immature phenotype for two days before harvesting.

2.4 Harvesting of Macrophages for Analysis

At day 9, the macrophages were harvested for further analysis. The culture plate was centrifuged, and supernatants were collected and centrifuged at 1000·g for 10 minutes at 4°C. Subsequently, the supernatants were aliquoted into Eppendorf tubes (stored at -80°C until use). MACS buffer was added to each well and incubated for 30 minutes at 4°C. Cells were collected, washed once with PBS, centrifuged and resuspended in medium followed by counting. Cell concentration was adjusted to 1×10^6 cells/ml.

2.5 Flow Cytometry

For phenotypic characterisation of the generated macrophages, two multicolor antibody panels were included, as stated in table 2.1. Initially, only a "*basic panel*" (Panel 1) was included and used for finding the optimal concentration of polarisation cytokines. Subsequently, Panel 2 was included. Prior to use, antibodies were titrated on positive cells (the phenotype with the assumption of the highest

CHAPTER 2. METHODS AND MATERIALS

expression of the marker). Panel 1 was titrated twice: once before the inclusion of Panel 2 and again at the same time as Panel 2. Prior to data acquisition of antibody titration on FACSLyric Flow Cytometer (BD Bioscience), stained cells were mixed with unstained cells. Data was analysed in FlowLogic (Inivai).

For flow analysis, 5×10^4 cells were seeded in in 96-wells plate (polypropylene), centrifuged and washed once with PBS. Cells were stained with Fixable Viability Stain 780 (FVS780) (1/4 of manufacturer's recommendation (BD Bioscience)) and incubated for 10 minutes 4°C. Cells were washed once in Flow Cytometry Staining Buffer (FACS) buffer, consisting of 10% FBS, 1mM EDTA (Region Hovedstadens Apotek) and 0.05% (weight/volume) Sodium Azide in PBS). Prior to staining with antibodies, the cells were blocked with FcBlock (10 ug/ml) (BD Bioscience) for 15 minutes at 4°C. Stained cells were incubated with antibodies for 30 minutes at 4°C and washed twice with FACS buffer. For intracellular staining, cells were fixated with Cytotfix/Cytoperm and washed with Perm/Wash (Fixation/Permeabilization Solution Kit, BD Bioscience). Stained and unstained cells were incubated overnight at 4°C in FACS buffer and flow cytometry was run the following day. Gating strategy for flow data is illustrated in figure 2.3. Data of the flow analysis included the percentage of cells positive for a given marker and delta-Median Fluorescence Intensity (MFI), meaning the MFI of stained cells minus MFI of unstained cells.

Table 2.1: An overview of the applied antibodies in the setup for flow cytometry and information regarding the antibody. Please note that the informed dilutions of the antibodies for panel 1 are based on the second antibody titration.

Panel 1				
Antibody	Fluorochrome	Clone	Dilution	Manufacturer
CD1a	PE	HI149	1/2x	BD Biosciences
CD14	Alexa Fluor 488	MøP9	1/2x	BD Biosciences
CD68	Brilliant Violet 421	Y1/82A	1/2x	BD Biosciences
CD209/DC-SIGN	APC	DCN46	1/4x	BD Biosciences
HLA-DR	PerCP-Cy5.5	G45-6	1/2x	BD Biosciences

Panel 2				
Antibody	Fluorochrome	Clone	Dilution	Manufacturer
CD38	BB515	HIT2	1/2x	BD Biosciences
CD85d/ILT4	APC	42D1	1/2x	Thermo Fisher Scientific
CD86	V450	2331 (FUN-1)	1/16x	BD Biosciences
CD163	PerCP-Cy5.5	GHI/61	1x	BD Biosciences
CD206	PE-Cyanine7	19.2	1/8x	Thermo Fisher Scientific

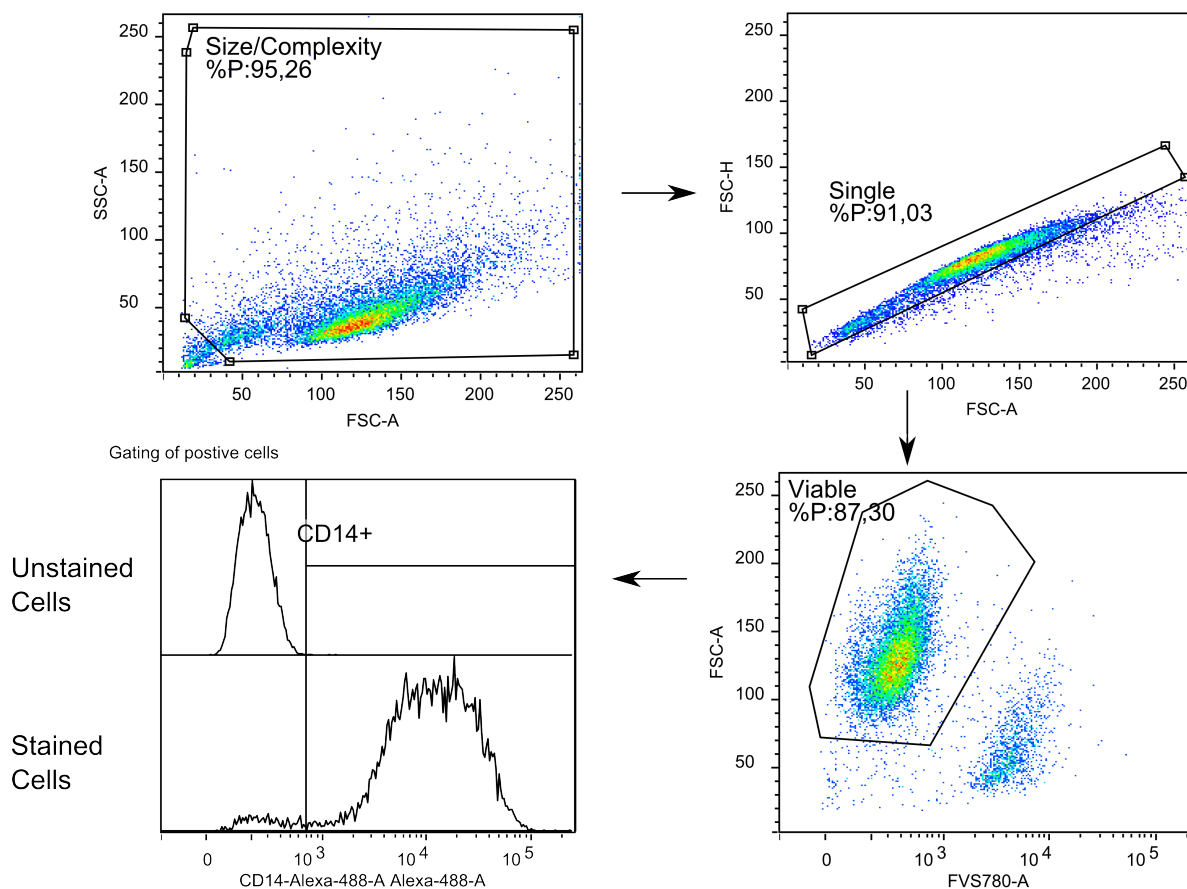


Figure 2.3: Illustrates the gating strategy for analysis of flow data of the surface markers. Initially, debris was removed from the analysis by gating size and complexity of the cells. Single cells were gated by using forward scatter height (FSC-H) versus forward scatter area (FSC-A) and were further gated for living cells. To remove background noise from the analysis, unstained and stained cells were plotted as a histogram. By gating on the fluorescence intensity located to the right of the unstained cells, cells were determined as positive for the respective marker, in this case CD14.

2.6 ELISA

Secretion of IL-10 (R&D Systems), IL-12p70 (R&D Systems) and TNF- α (R&D Systems) was measured by ELISA (DuoSet ELISA kits, R&D Systems), according to the instruction of the manufacturer. Optimal dilution of supernatants was determined to ensure that the factors were within detection range. The ELISA plate was read on FLUOstar Omega microplate reader (BMG labtech) with absorbance at 450 nm and subtraction at 540 nm. Experiments were performed in duplicates. The concentrations detected by ELISA were determined by 4-parameter curve-fitting of blank corrected absorbance values.

2.7 Phagocytosis Assay

The phagocytotic properties of macrophages were assessed by phagocytosis of fluorescent (Crimson 625/645 nm) Carboxylated-Modified Microspheres (size of $1\mu\text{m}$), hereinafter referred to as beads (Invitrogen, Thermo Fisher Scientific), illustrated in figure 2.4.

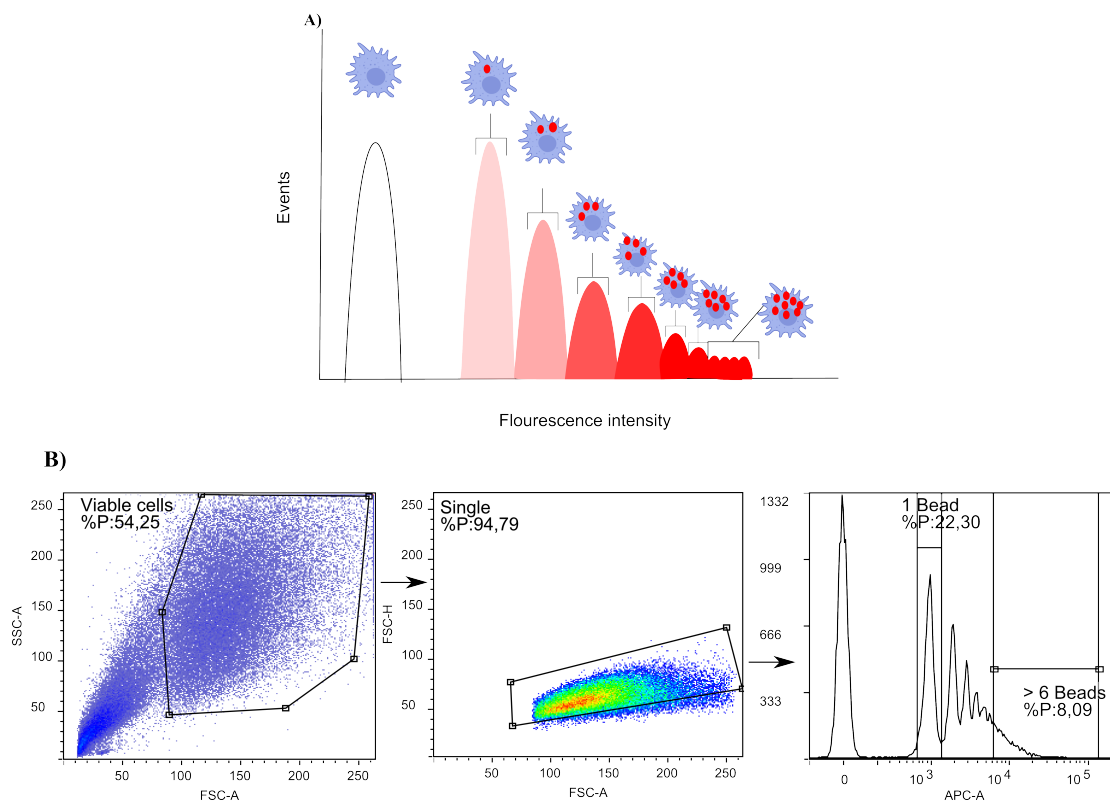


Figure 2.4: **A:** Illustration of beads phagocytised by macrophages. The measured fluorescence intensity increases with the number of beads phagocytised by the macrophages. In detail, the first peak, with a fluorescence intensity greater than one, indicates the number of macrophages, which have phagocytised one bead. The second peak indicates number of macrophages, which have phagocytised two beads, and so on. **B:** Illustration of the gating strategy for analysis of phagocytosis data. Initially, viable cells were gated by size and complexity. Forward scatter height (FSC-H) versus forward scatter area (FSC-A) was applied to discriminate doublet cells from single cells. Viable, single cells were used for the analysis. The number of beads phagocytised by macrophages were determined by gating on every peak of the fluorescence intensity. However, it is difficult to discriminate macrophages, which have phagocytised more than six beads. Therefore, above six beads have been gated as one gate.

Prior to use, the beads were shaken thoroughly for few minutes. 1×10^5 macrophages were seeded in round bottom 96-well plate (polypropylene) (Corning). A bead concentration of 1.9×10^9 beads/ml was generated by dilution in medium and was incubated at 37°C , 5% CO_2 (HERA cell 150)

for 30 minutes. The macrophages were incubated 37°C, 5% CO₂ (HERA cell 150) for 16 hours with 1×10^7 beads/ml. The optimal bead concentration was determined by titration of the beads. The optimal exposure time of macrophages for beads was determined by harvesting the cells, exposed to beads, at different time points, elaborated in results (see section 3.6). Prior to flow analysis on FACSLyrics Flow Cytometer (BD Bioscience), the plate was centrifuged and cells were resuspended in FACS buffer. The gating strategy for analysis of phagocytosis data is illustrated in figure 2.4. From these data, the number of phagocytising cells were determined, as well as beads per cell and beads per phagocytising cell. Beads per phagocytising cell were calculated by MFI of all phagocytising cells divided by MFI of one bead.

In order to validate the beads phagocytised by macrophages using microscopy, remaining cells were fixated in 4% paraformaldehyde (Region Hovedstadens Apotek), immediately after flow cytometric data acquisition. Cells were washed in PBS and permeabilised in 0.1% Triton-X (Producent) PBS for 30 minutes before staining of actin filaments with Alexa Fluor 568 Phalloidin (Invitrogen, Thermo Fisher Scientific) and nuclei by 4',6-Diamidino-2-Phenylindole, Dilactate (DAPI) (Molecular Probes, Thermo Fisher Scientific) according to manufacturers instructions. Following staining, the cells were centrifuged and resuspended in 10 ul of ddH₂O and transferred to Superfrost Plus microscope slides (Menzel-Gläser, Thermo Scientific). The small volume was allowed to evaporate partially before addition of 10 ul ProLong Diamond Antifade Mountant (Invitrogen, Thermo Fisher Scientific) and careful placement of #1.5 cover slip. The samples were imaged as maximum intensity projections of Z-stacks on a Zeiss Axio Observer 7, using a Plan-Apo 100x/1.4 Oil (PH3) objective (Zeiss).

2.8 Mixed Lymphocyte Reaction Assay

The ability of macrophages to induce proliferation of allogeneic lymphocytes was investigated on PMBC as responder cells. Four PMBC donors, were isolated from buffy coats as described in section 2.1. Cells were resuspended in cryomedium consisting of 10% DMSO in FBS, and aliquoted into cryotubes (Thermo Fisher) at a cell concentration of 1×10^7 cells/ml. Initially, the cells were frozen in CoolCell overnight in -80°C for controlled freezing, before storage in liquid nitrogen.

At day 10, PMBC was thawed in waterbath (37°C) for 10 minutes and recovered in medium (1:10 dilution) in the incubator for one hour followed by centrifugation at 500·g for 5 minutes. PMBC

were labeled with 5 μ M Carboxyfluorescein succinimidyl ester (CFSE) (BD Bioscience) in PBS-FBS solution (PBS and 2.5% FBS) for 10 minutes in waterbath (37°C). The cells were washed twice in a PBS-FBS solution (PBS and 5% FBS) and resuspended in medium for cell counting and seeding. 1×10^5 PMBC were seeded in round bottom 96-wells plate (polystyrene, Corning), where 2×10^4 macrophages were seeded (a ratio at 1:5 (macrophage:PMBC)). If there was a sufficient number of cells, the experiment was performed in duplicates.

2.8.1 Flow Cytometry for Mixed Lymphocyte Reaction Assay

At day 15, 5 days after initiation of Mixed Lymphocyte Reaction (MLR), the plate was centrifuged and cells were resuspended in PBS for staining with FVS780 (1/4 of manufacturer's recommendation (BD Bioscience)). The cells were incubated dark at 4°C for 15 minutes followed by two washing steps with FACS buffer. Duplicates were pooled immediately prior to flow analysis. The gating strategy for MLR data is illustrated in figure 2.5. For further analysis, four statistical analyses have been applied to describe the cellular proliferation: Fraction Diluted (Dil/P), Replication Index (RI), Division Index (DI) and Precursor Frequency (PF). Dil/P describes the fraction of cells in the final population which have divided at least once. RI quantifies the number of responder cells in the end of culture divided by the number of proliferating cells in the starting population. DI denotes the average number of divisions of cells in the culture. PF is the fraction of the starting population which has divided at least once [41].

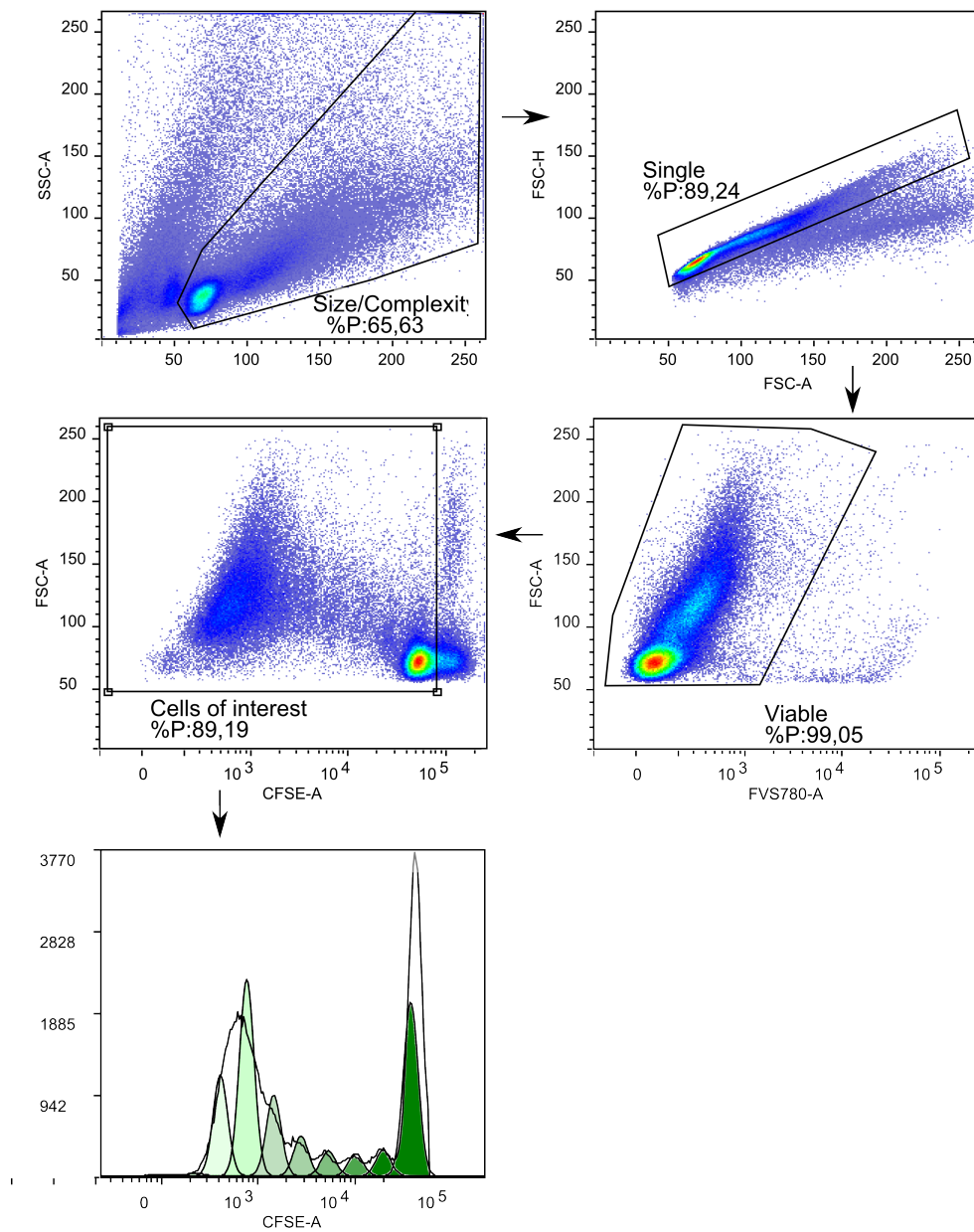


Figure 2.5: Illustrates the gating strategy for MLR. Initially, the macrophages and responder cells were gated by size and complexity of the cells. Forward scatter height (FSC-H) versus forward scatter area (FSC-A) was applied to discriminate doublet cells from single cells. Viable cells was gated for further analysis gating cells, which is negative for FVS780. Cells of interest were gated before fitting of proliferating cells.

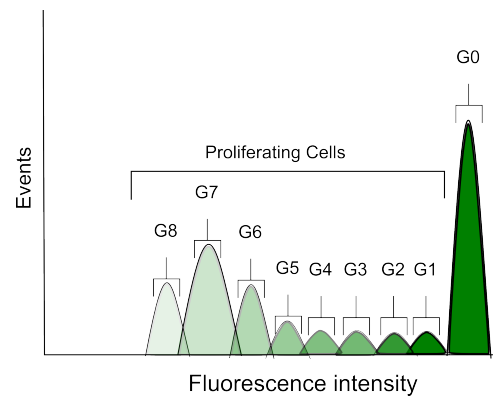


Figure 2.6: Illustrates divisions of cells in the culture. The fluorescence intensity decreases as the cells proliferate. G1 indicates the number of cells, which have divided once, where G2 indicates the number of cells, which have divided twice, and so on.

2.9 Data analysis and Figures

Graphs, data and statistical analysis have been performed in SPSS (IBM, version 25). Data was tested for normal distribution by Shapiro-Wilk's test. If the requirement of normally distributed data was met, a parametric Paired Sample test was performed, if not, a non-parametric Wilcoxon Signed Rank Test was performed. The level of significance was set at $p=0.05$. For multiple comparisons, p 's were adjusted by Bonferroni correction. Figures were made in BioRender or Inkscape.

3 Results

3.1 Cytokine Titration

As generation of monocyte-derived macrophages relies on polarising cytokines, GM-CSF and M-CSF were titrated in a 2-folds dilution ranging from 100 ng/ml to 3.125 ng/ml, in order to find the optimal concentration for generation of M1 and M2 macrophages, respectively. In general, CD1a and CD209 (DC-SIGN) are associated markers for DC [42, 43], whereas high expression of CD14, CD68, and HLA-DR are phenotypical markers for macrophages [28, 30, 31].

3.1.1 M1 Macrophages: Titration of GM-CSF

The number of viable M1 macrophages was in general the same or higher than seeded cells, represented by the black line in figure 3.1A, indicating that viability of M1 macrophages was independent of concentrations of GM-CSF ranging from 100 ng/ml to 3.125 ng/ml. No major differences were observed in the expression of each marker (in Panel 1) between the different concentrations of GM-CSF (figure 3.1B and C). As expected, the expression of CD1a and CD209 were low whereas the expression of CD14, CD68 and HLA-DR were high. These results indicate that generation of M1 macrophages from CD14⁺ monocytes in presence of GM-CSF is independent of the concentration of GM-CSF. Therefore, it was decided to polarise CD14⁺ monocytes into M1 macrophages with 10ng/ml GM-CSF.

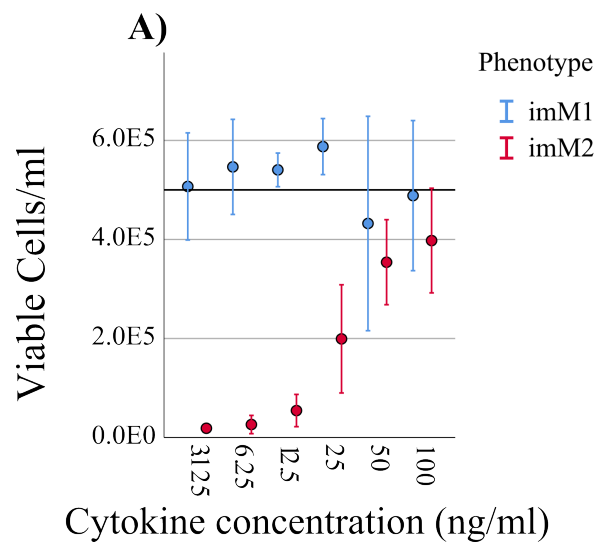
3.1.2 M2 Macrophages: Titration of M-CSF

The viability of M2 macrophages decreased with decreasing concentration of M-CSF, indicating that the viability of M2 macrophages *in vitro* is dependent on the concentration of M-CSF (figure 3.1A).

Similar to M1 macrophages, the expression of CD1a was low, but contrarily, the M2 macrophages had a higher expression of CD209, which increased with increasing concentration of M-CSF (figure 3.1B and C). As mentioned, CD14, CD68 and HLA-DR are well known markers for macrophages and therefore the optimal concentration of M-CSF should be determined by the highest expression of these markers, except from HLA-DR, since a fully polarised M2 macrophage has lower expression of HLA-DR [44]. Interestingly, the expression level of CD68 decreased at higher concentration of

M-CSF. Additionally, the level of expression of each marker was dose-dependent of M-CSF (figure 3.1C). No major differences of the expression of CD14, CD68, HLA-DR and CD209 were observed at higher concentration of M-CSF (50 ng/ml and 100 ng/ml). Based on viability, expression of CD14 and HLA-DR, it was determined to differentiate CD14⁺ monocytes with a concentration of 75 ng/ml M-CSF to generate M2 macrophages.

These results show that two distinct immature phenotypes of macrophages have been generated from CD14⁺ monocytes. The morphological development during differentiation of the M1 and M2 macrophages is illustrated in figure 3.6 and will be addressed later in section 3.4.



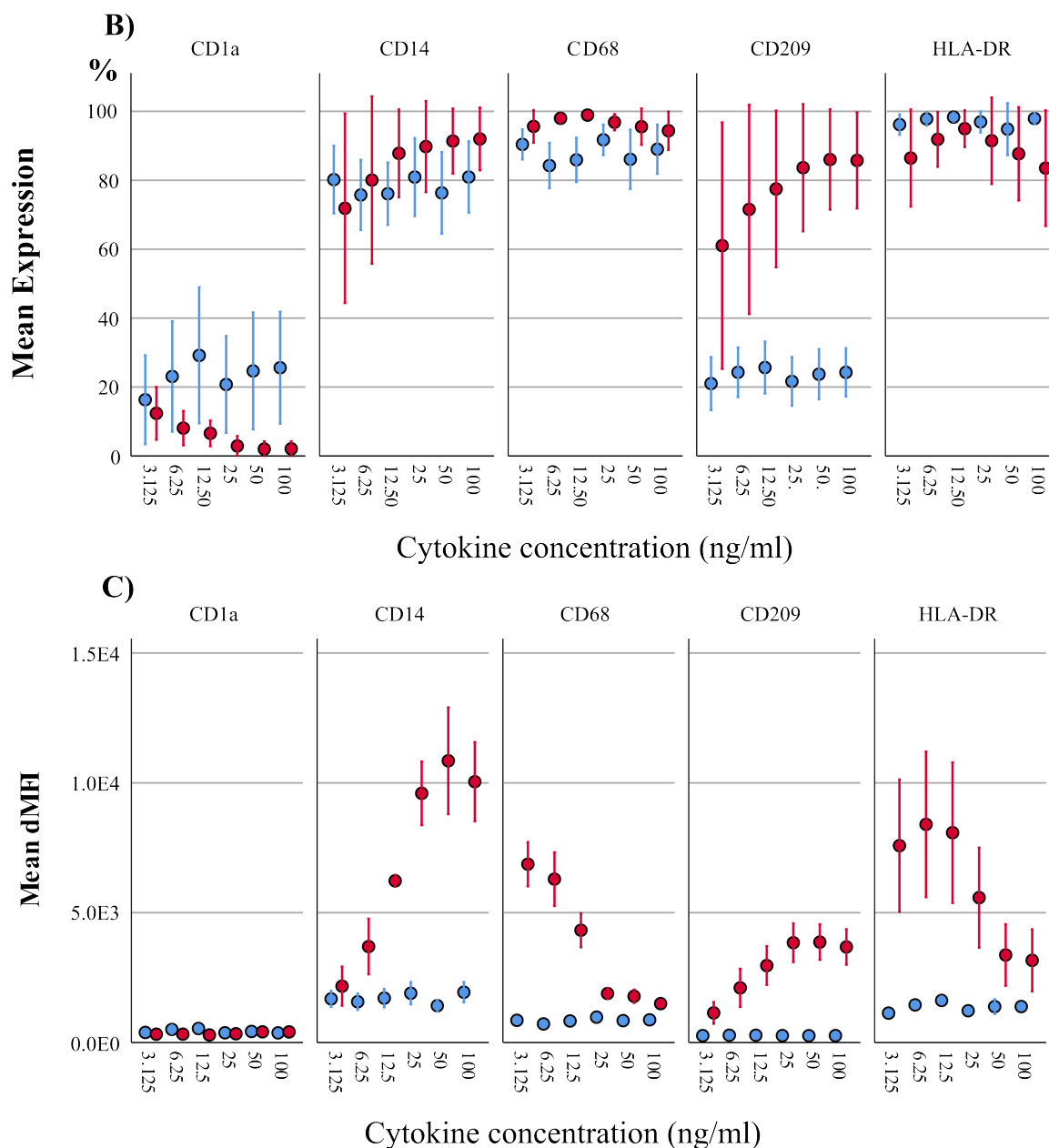


Figure 3.1: **A)** Viable cells per milliliter for immature M1 (blue) and M2 (red) macrophages, when polarised with different concentrations of the polarisation cytokines, GM-CSF and M-CSF, respectively. The black line indicates the number of cells seeded. **B)** Portion of imM1 and imM2 macrophages, which positively expressed a marker of Panel 1, at different concentrations of GM-CSF and M-CSF, respectively. **c)** Average dMFI of each marker in Panel 1, when polarised with different concentrations of GM-CSF and M-CSF, respectively. dMFI: delta Median Fluorescence Intensity. imM1: n=4 imM2 n=4, ± 1 SE

3.2 Cell Seeding Density

The optimal seeding density was determined by seeding immature cells at different cell concentrations ranging from 1×10^5 to 6×10^5 cells/ml in activating medium consisting of 100 ng/ml LPS in com-

ination with 20 ng/ml IFN- γ and 20 ng/ml IL-4 for generation of mature M1 and M2a macrophages, respectively.

It appeared that the number of viable cells per milliliter for mM1 and M2a macrophages reach a plateau when cells were seeded at a concentration of 4×10^5 and 5×10^5 cells per milliliter, indicated by the red (mM1), blue (M2a) and the dotted line (representing the mean of all data points) in figure 3.2. This suggested the presence of limiting factors impacting the viability of cells, which was undesirable in this setup. Therefore, cells seeded above 4×10^5 cells per milliliter can be excluded from the set of optimal seeding densities. Conclusively, it was preferred to harvest as many viable cells as possible and, additionally, to treat the phenotypes as equally as possible. This resulted in that the generated phenotypes were seeded at a concentration of 3.5×10^5 cells per milliliter for activation.

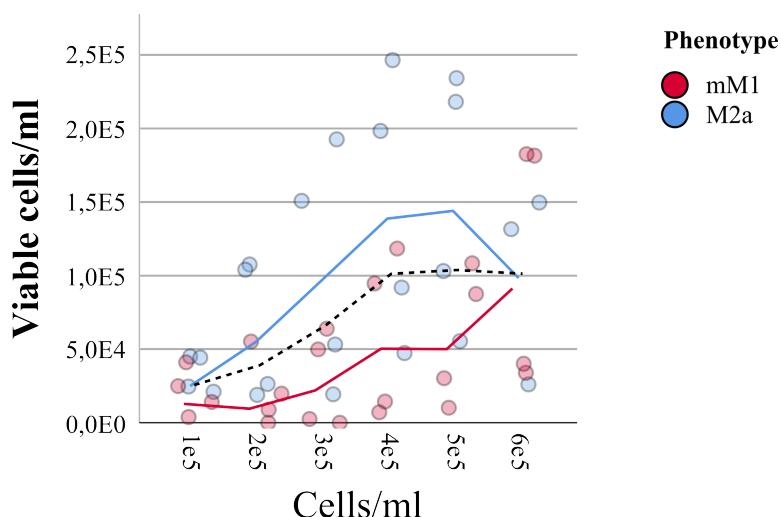


Figure 3.2: The number of harvested viable cells per milliliter for mM1 (red) and M2a (blue) macrophages, when seeded at different concentrations and activated with activating stimuli for two days (M1: 100 ng/ml LPS and 20 ng/ml IFN- γ and M2a: 20 ng/ml IL-4). The black dotted line indicates the average of harvested viable cells of both phenotypes. $n=4$

3.3 Titration of Activating Stimuli

After determination of the cell seeding density for activation of the macrophages, the activating stimuli were titrated in order to find the optimal concentration for generation of mature phenotypes: mM1, M2a and M2c. For flow cytometry an additional panel (Panel 2) was designed and optimised in an effort to distinguish the mature phenotypes from each other.

3.3.1 Maturation of M1 macrophages

The fully mature M1 macrophage was generated by activation with LPS in combination with IFN- γ . Initially, LPS was titrated to find the optimal concentration followed by titration of IFN- γ while the concentration of LPS was held constant at optimum.

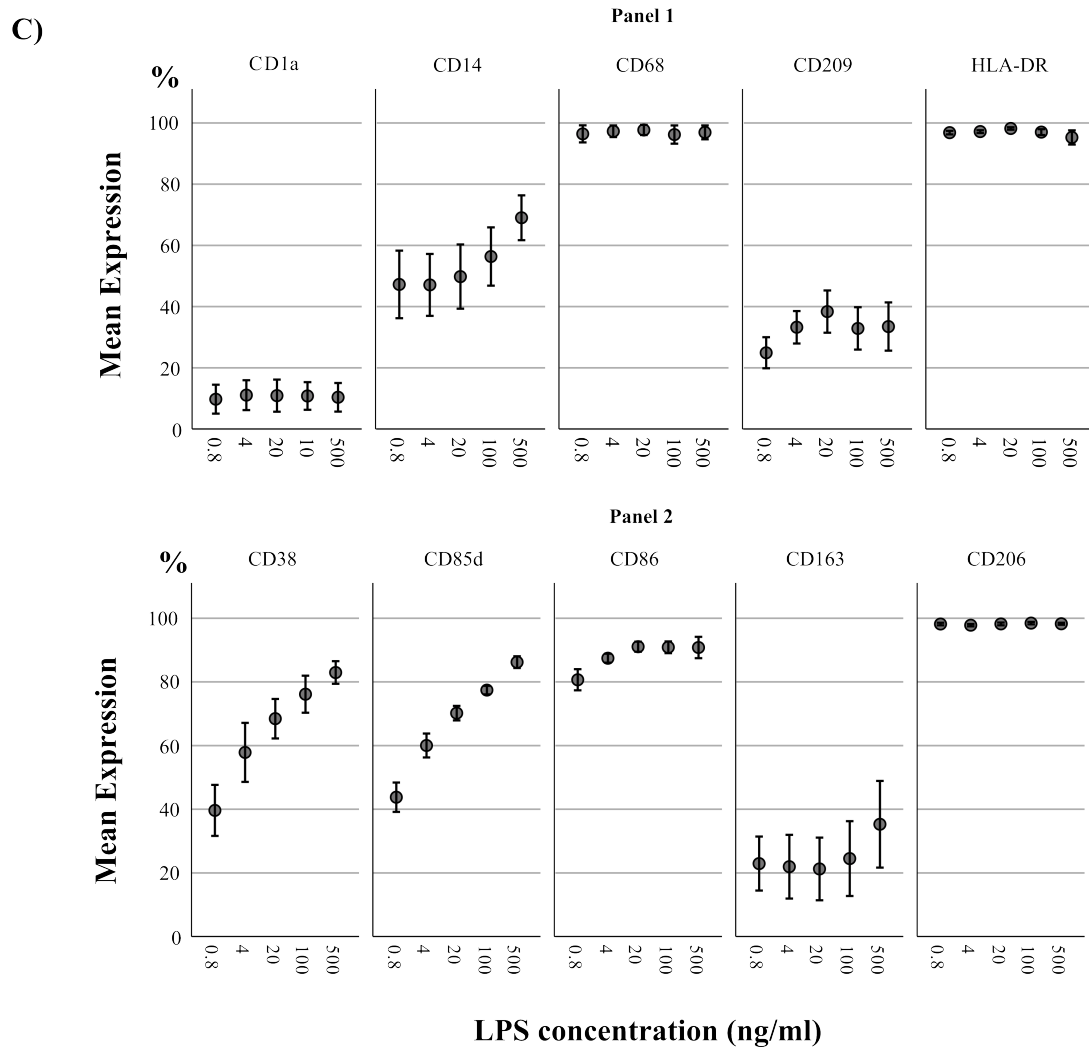
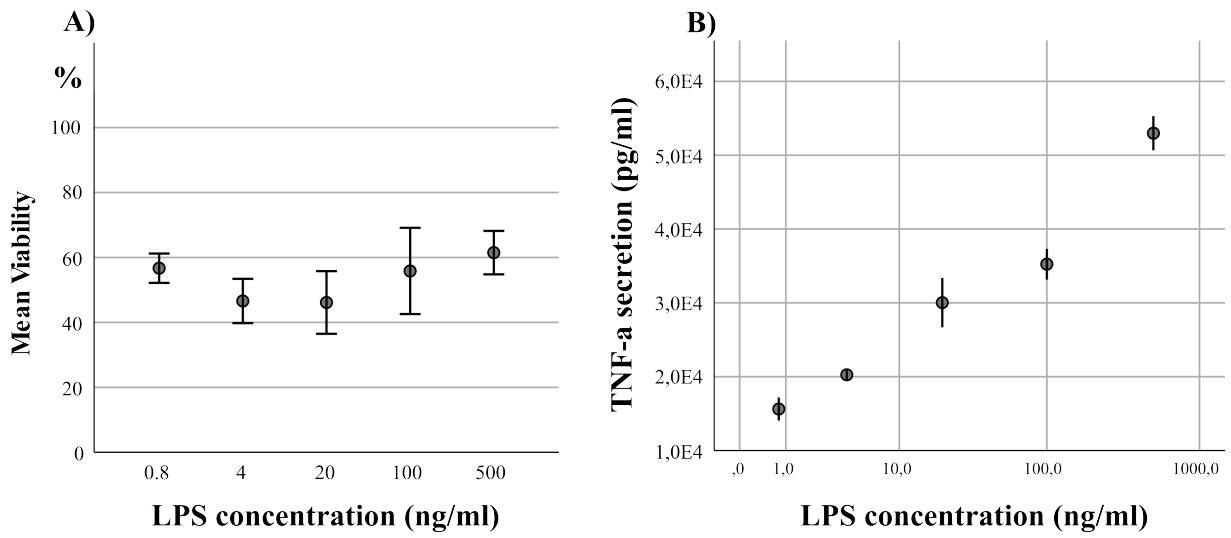
3.3.1.1 Titration of LPS

LPS was titrated in a 5-folds dilution ranging from 500 ng/ml to 0.8 ng/ml. The viability of macrophages decreased when exposed to LPS. However, toxicity in response to increased concentration of LPS was not observed (figure 3.3A).

The secretion of TNF- α by LPS activated M1 macrophages increased with increasing concentrations of LPS (figure 3.3B). Secretion of IL-12p70 was undetectable (data not shown).

More cells expressed CD14, CD38, CD85d, CD86 and CD163 with increasing concentration of LPS. However, the expression of CD1a, CD209 and CD163 was considered low compared to the other markers (figure 3.3C). These results were in general supported by data for dMFI (3.3D). Additionally, all cells expressed CD68, HLA-DR, CD86 and CD206 (figure 3.3C), however, the level of expression of the marker showed different patterns. HLA-DR and CD86 reached the highest expression at a concentration of 20 ng/ml LPS. The expression of the markers decreased slightly with higher concentration of LPS. The level of expression of CD68 and CD206 decreased in a dose-dependent manner (figure 3.3D).

Based on these findings the optimal concentration of LPS was 500 ng/ml.



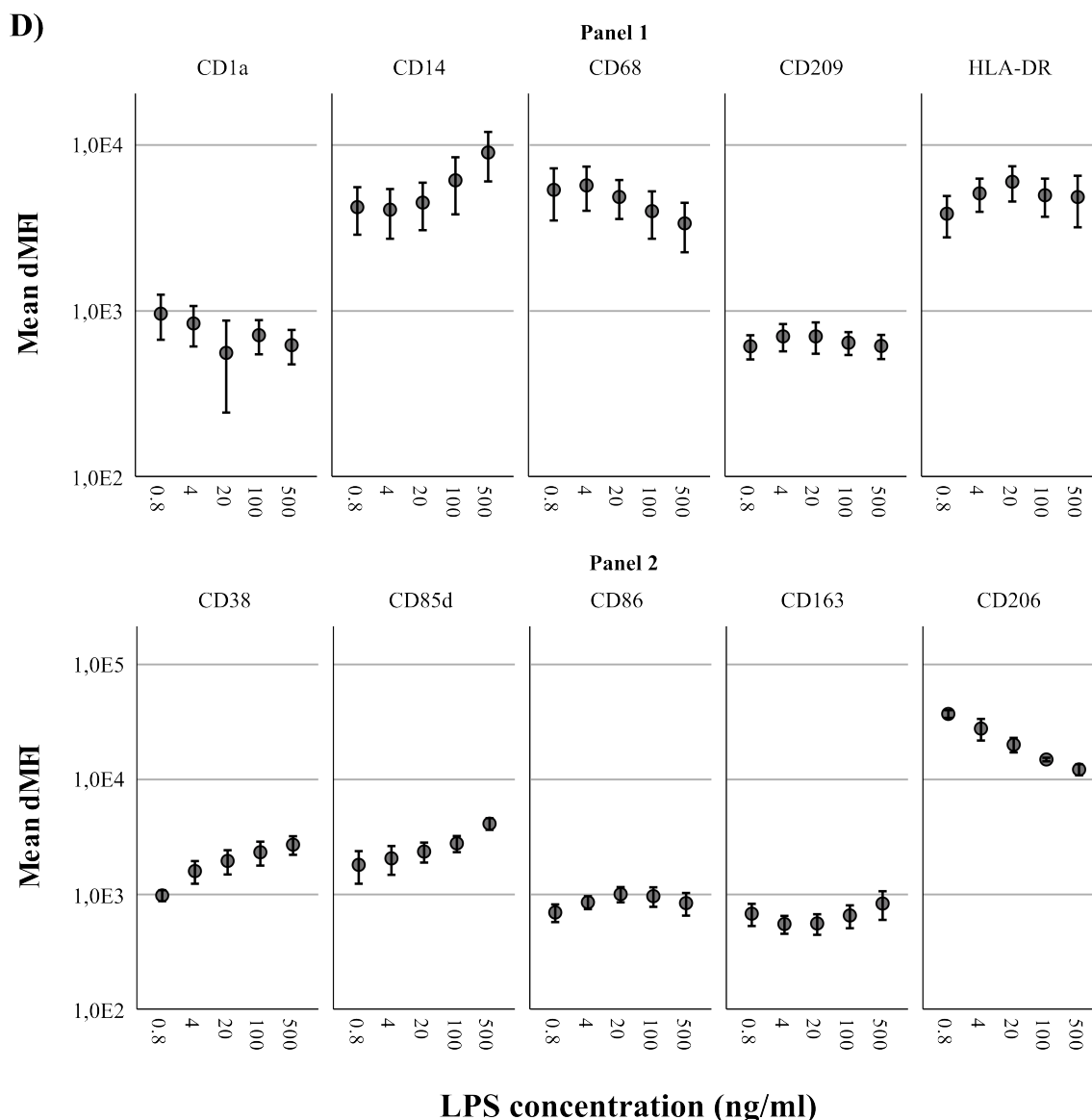


Figure 3.3: **A)** Viability in percent of M1 macrophages activated with different concentrations of LPS. **B)** Mean secretion of TNF- α (pg/ml) secreted by M1 macrophages activated with different concentrations of LPS. **C)** The portion of M1 macrophages which positively expressed a marker of Panel 1 and Panel 2. **D)** Mean dMFI of each marker in Panel 1 and Panel 2, when activated with the different concentrations of LPS. dMFI: delta Median Fluorescence Intensity. n=3, \pm 1 SE

3.3.1.2 Titration of IFN- γ

IFN- γ was titrated in a 4-folds dilution ranging from 80 ng/ml to 0.3125 ng/ml in combination with LPS at a concentration of 500 ng/ml.

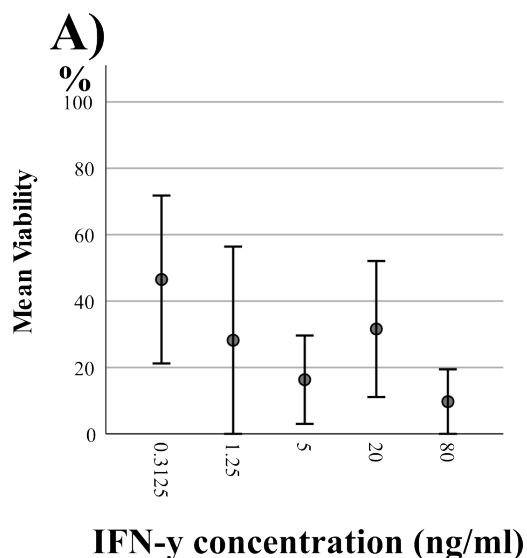
The viability of cells was in general low and decreased in response to increased concentration of IFN- γ (figure 3.4A). These results led to reconsideration of the method for harvesting the cells and additional experiments, described in appendix 5.2. These results illustrated that no differences

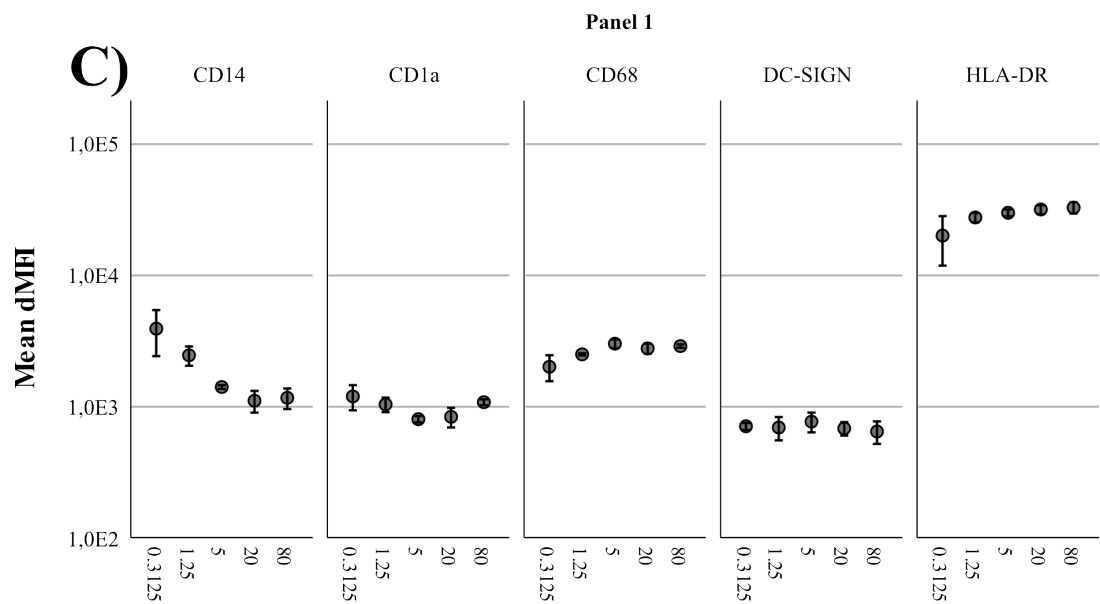
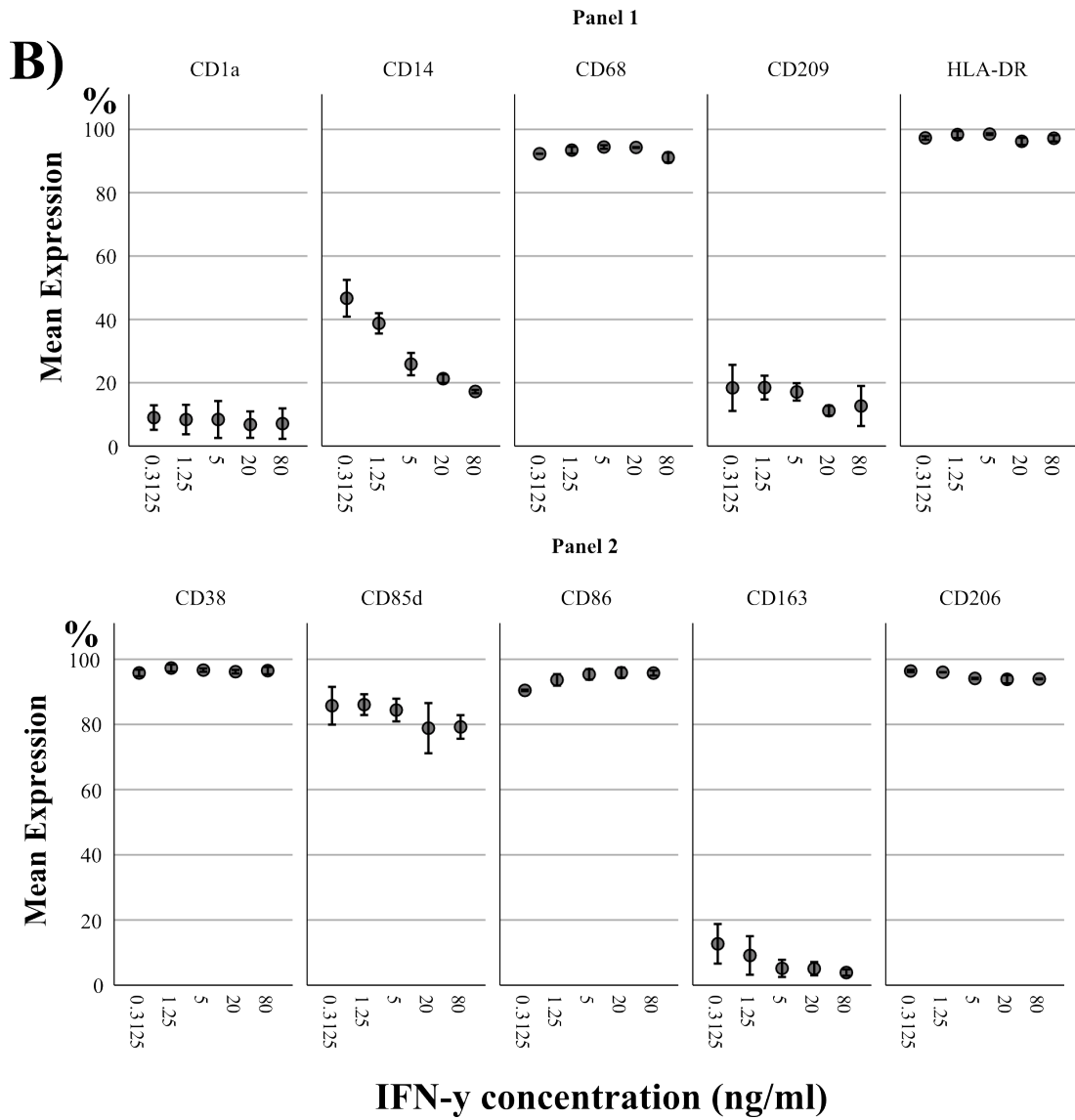
in toxicity was observed between 100 ng/ml LPS and 500 ng/ml LPS in combination with IFN- γ . Reassured, the practice of activating M1 macrophages with 500 ng/ml LPS was continued.

Interestingly, the number of cells expressing CD14 and the expression level decreased with higher concentration of IFN- γ . The pattern for CD85d was similar to CD14, just to a lesser extent (figure 3.4B and C). Approximately, all the cells expressed CD38, CD68, HLA-DR, CD86 and CD206 (figure 3.4B). However, the level of expression varied between concentration of IFN- γ . The expression of CD206 decreased whereas the expression of CD38, CD86 and HLA-DR increased slightly with increasing concentration of IFN- γ (figure 3.4C).

The secretion of IL-12p70 increased remarkably until 5 ng/ml IFN- γ where the secretion reached a plateau. The highest secreted amount of TNF- α was observed when activated with 5 ng/ml IFN- γ . Additionally, the secretion of TNF- α was several magnitudes higher than the secretion of IL-12p70 (figure 3.4D).

Conclusively, a desirable mature M1 macrophage is characterised by high expression of CD38, CD86 and HLA-DR [24, 32] accompanied by secretion of IL-12 and TNF- α [33] and low(er) expression of CD14 and CD206. This desirable phenotype was generated by activation with 5 ng/ml IFN- γ in combination with 500 ng/ml LPS.





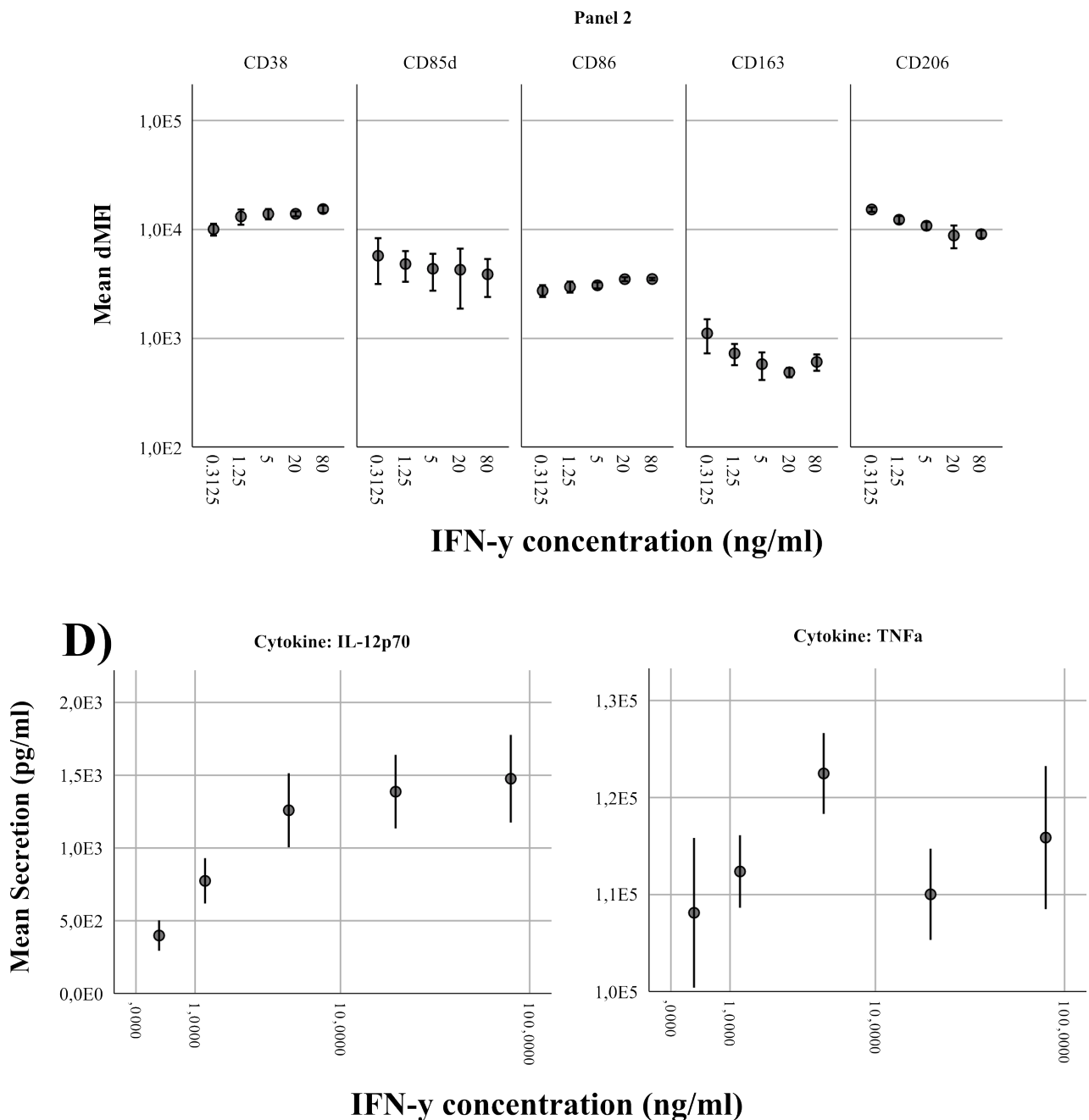


Figure 3.4: **A)** The viability in percent of M1 macrophages activated with 500 ng/ml LPS for varying concentrations of IFN- γ . **B)** The percentage of the activated M1 macrophages expressing a specific marker of Panel 1 and Panel 2 at a given concentration of IFN- γ in combination with LPS. **C)** Mean dMFI of each marker in Panel 1 and Panel 2, when activated with the different concentrations of IFN- γ in combination with LPS. **D)** Mean secretion of IL-12p70 and TNF- α (pg/ml) secreted by M1 macrophages activated with 500 ng/ml LPS for varying concentrations of IFN- γ . dMFI: delta Median Fluorescence Intensity. n=3, \pm 1 SE

3.3.2 Maturation of M2a macrophages

M2a macrophages were generated by activation with IL-4. To find the optimal concentration, the cytokine was titrated in a 4-folds dilution ranging from 80 ng/ml to 0.3125 ng/ml.

The viability of maturation of M2a macrophages was not affected by the concentration of IL-4 (in figure 3.5A).

Increasing concentration of IL-4 resulted in fewer cells expressing CD14 and CD163, while more cells expressed CD209 (figure 3.5C). According to dMFI for all markers, there was observed little to no difference in the level of expression, except from the expression of CD85d and CD163 which decreased slightly with increasing concentration of IL-4 (figure 3.5D). CD206, an important marker for distinction of M2a and M2c subtypes [34], was positively expressed on all M2a macrophages with no difference in dMFI (figure 3.5C and D). This indicated that the M2a phenotype can be generated independently of the concentration of IL-4. The concentration of IL-4 did not impact the secretion of IL-10 by M2a macrophages (figure 3.5B).

Conclusively, it was determined to activate immature M2 macrophages with 20 ng/ml IL-4 to generate M2a macrophages.

3.3.3 Maturation of M2c macrophages

M2c macrophages were generated by activation with IL-10. To find the optimal concentration, the cytokine was titrated in a 4-folds dilution ranging from 80 ng/ml to 0.3125 ng/ml.

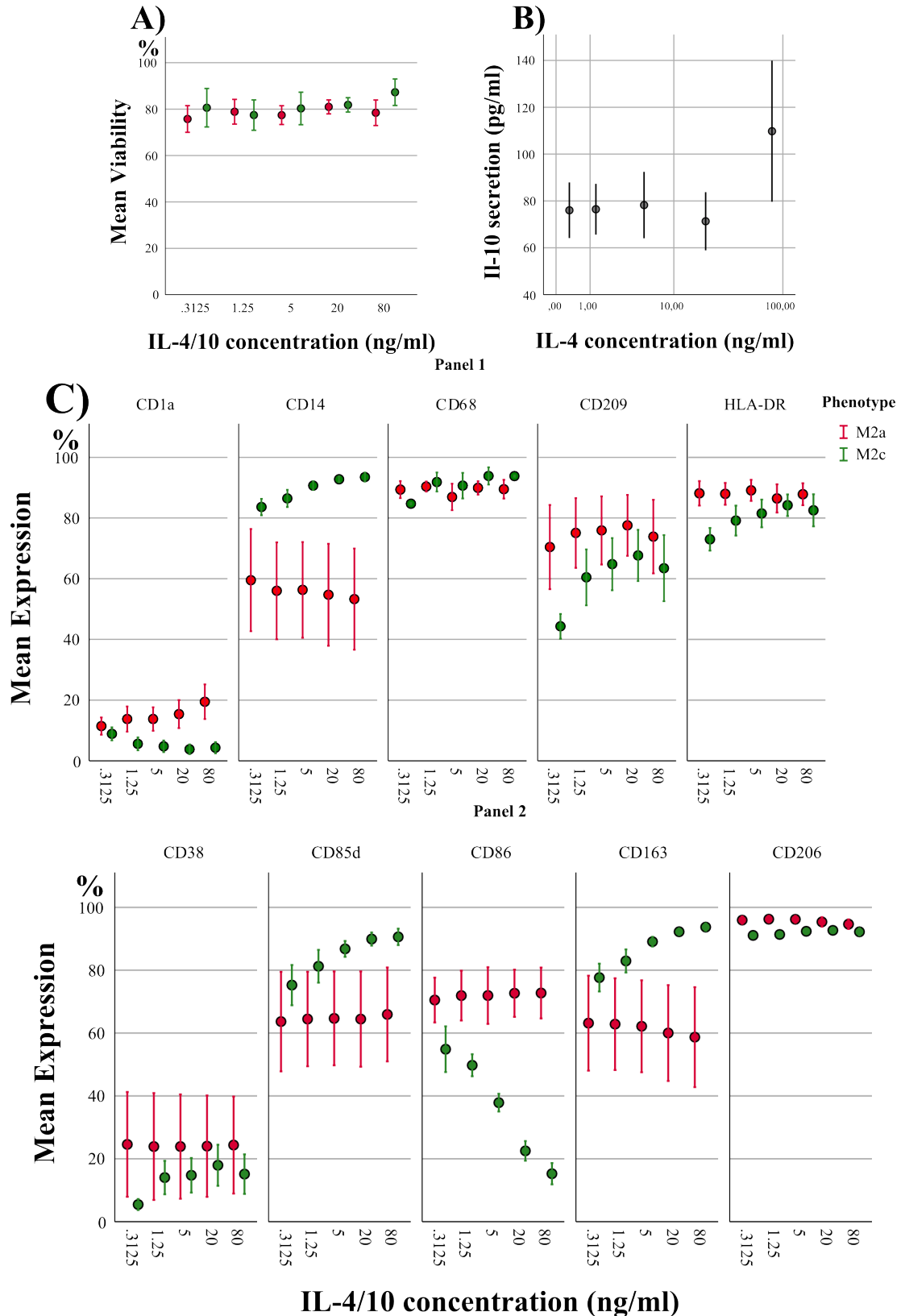
The concentration of IL-10 did not impact the viability of generated M2c macrophages (figure 3.5A).

The number of cells expressing CD14, CD209, HLA-DR, CD85 and CD163 increased with an increasing concentration of IL-10, while the number of cells expressing CD86 decreased (figure 3.5C). These findings were supported by data of dMFI. Additionally, little to no difference of the level of expression of CD68 and CD206 was observed between the different concentrations of IL-10 (figure 3.5D). Furthermore, the secretion of IL-10 was attempted measured ELISA (data shown in appendix, figure 5.3). However, data was ambiguous since the immature macrophages were activated with IL-10 and the activating cytokine was measured as well.

Conclusively, the optimal concentration of IL-10 for generation of M2c macrophages was 40

CHAPTER 3. RESULTS

ng/ml, based on low(er) expression of pro-inflammatory markers such as CD38, CD86 and HLA-DR and high expression of CD163, which is suggested to be a marker for M2c macrophages [33–35].



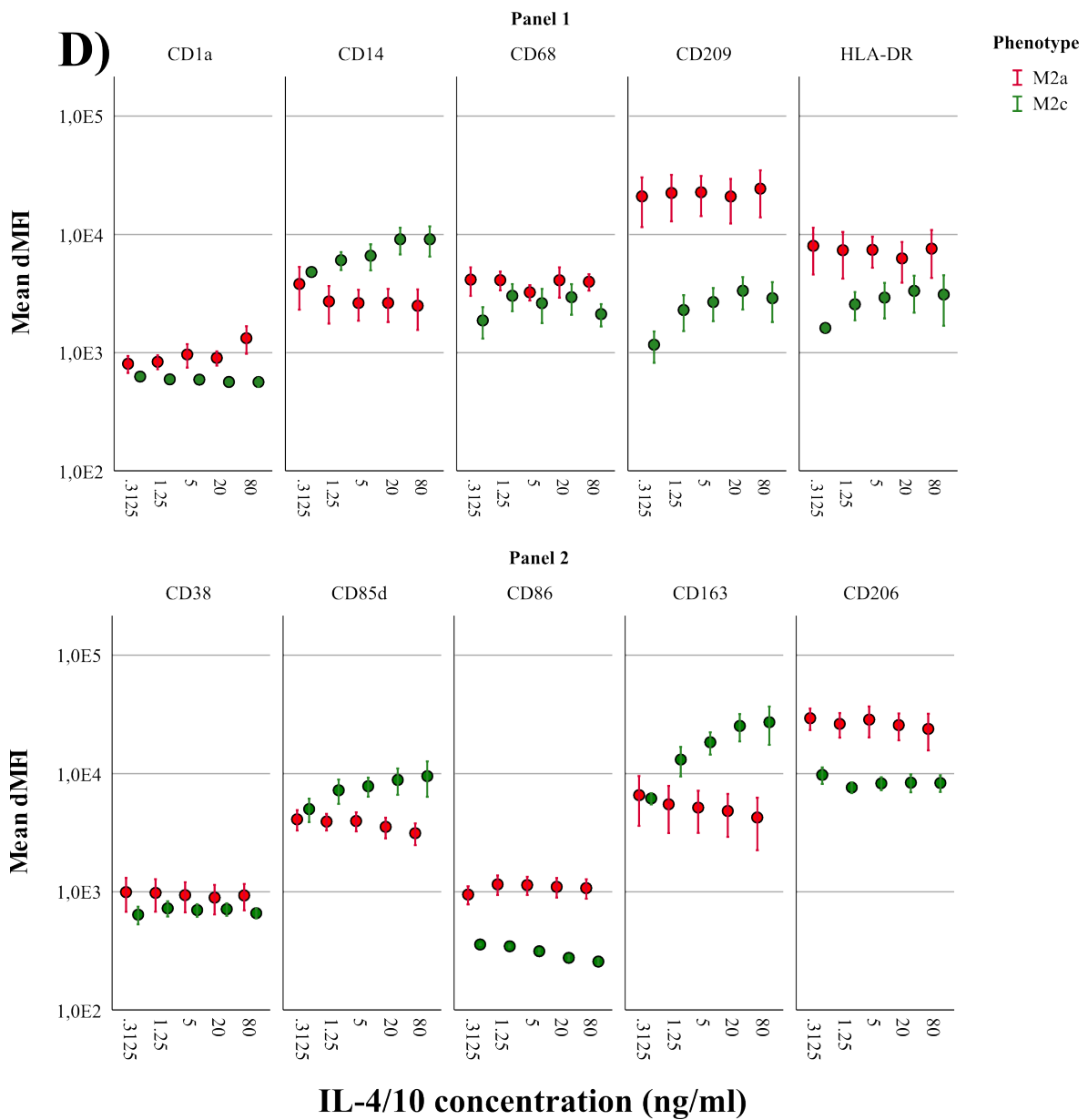


Figure 3.5: **A)** Viability of M2a (red) and M2c (green) macrophages when activated with different concentration of IL-4 and 10, respectively. **B)** Mean secretion of IL-10 secreted by M2a macrophages, when activated with different concentrations of IL-4. **C)** Percent of the M2a and M2c macrophages which positively expressed a marker of Panel 1 and Panel 2. **D)** Mean dMFI of each marker in Panel 1 and Panel 2, when activated the different concentrations of activating stimuli. dMFI: delta Median Fluorescence Intensity. M2a: n=5 M2c n=4, ± 1 SE

3.4 Morphological Characteristics and Expression of Markers

From newly isolated monocytes to fully differentiated mature macrophage phenotypes, the cells underwent substantial morphological changes as illustrated in figure 3.6. Initially, the cells were small and round but over time they increased in size and complexity. The immature M1 macrophage had a flattened, egg-shaped appearance, whereas some immature M2 macrophage took on a more spindle-shaped form while others maintained the egg-shaped morphology. The mature M1 macrophages became more star-shaped with protrusions, while the M2a and M2c macrophages were elongated or egg-shaped. Additionally, M2c macrophages appeared to contain higher content of vacuoles compared to mature M1 and M2a macrophages. The marker expression of the various generated immature and mature phenotypes are distinguishable from each other and monocytes (shown in appendix 5.1), as illustrated in table 3.1 and figure 3.7.

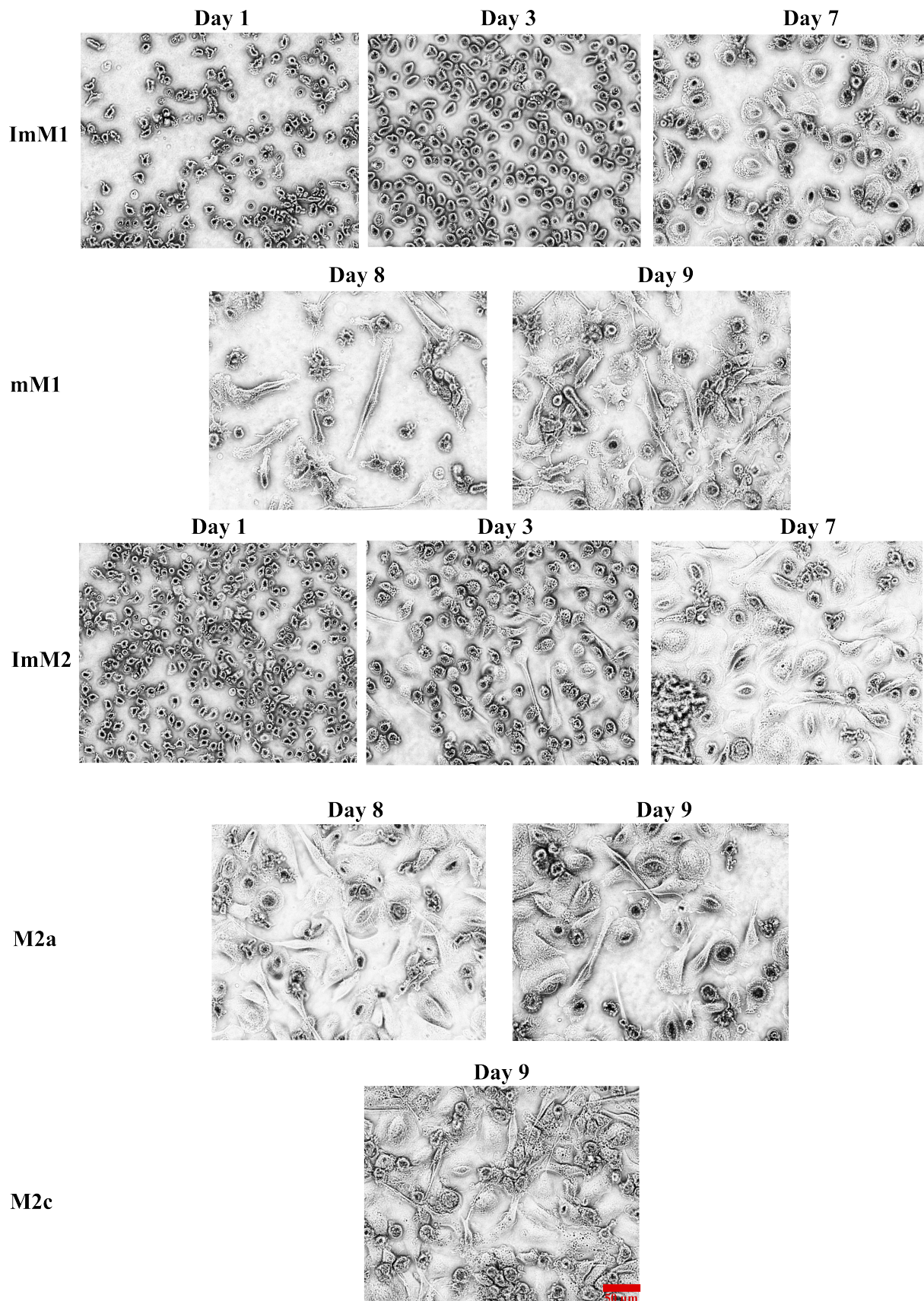


Figure 3.6: The morphological development of monocytes to immature and mature macrophages over time. The red line indicates the length of 50 μm

Table 3.1: An overview of the marker expression on monocytes, immature and mature phenotypes of macrophages. Marker expression is divided into four groups: -, +, ++ and +++, which indicates the degree of the expression of the marker. -: 0-24 %, +: 25-49 %, ++: 50-74 % and +++: 75-100 % marker expression. Monocytes: n= 4, Immature M1 n= 8, Mature M1: n=10, M2a: n= 4 and M2c: n=3

Phenotype	Monocyte	M1		M2		
		Immature	Mature	Immature	M2a	M2c
CD1a	-	-	-	-	-	-
CD14	++	+	+	+++	++	+++
CD38	+++	-	+++	+	-	++
CD68	++	+++	+++	+++	++	+++
CD85d	+++	+	+++	+++	+++	+++
CD86	-	++	+++	-	++	-
CD163	+	+	-	+++	++	+++
CD206	-	+++	+++	+++	+++	+++
CD209	-	-	-	+	+++	+
HLA-DR	+++	+++	+++	++	+++	+

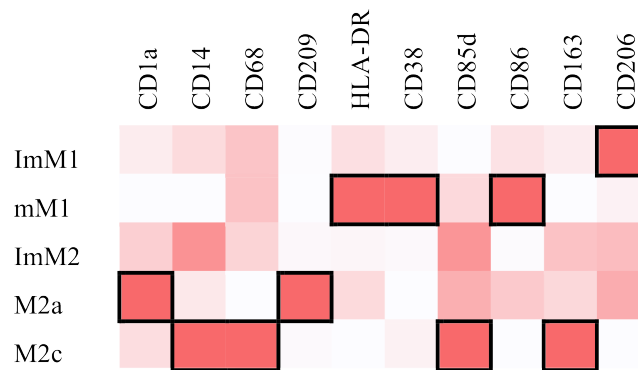


Figure 3.7: The level of expression of markers for each generated phenotype illustrated as a heatmap. The intensity of the red colour represents the expression level of a marker on the given phenotype (light red: low expression, red: high expression). The black boxes represent the phenotype with highest expression of marker(s) compared to the other phenotypes.

3.5 AT-MSc ratio

Prior to investigation of the immunomodulatory properties of AT-MSc on macrophages, the optimal concentration of AT-MSc was determined by seeding different concentrations of AT-MSc in the culture with M1 macrophages (Ratios: 1:5, 1:10, 1:20 and 1:40 (AT-MSc:macrophage)) either in juxtacrine or paracrine co-culture. The cells were activated for two days as described in method section 2.3.2.

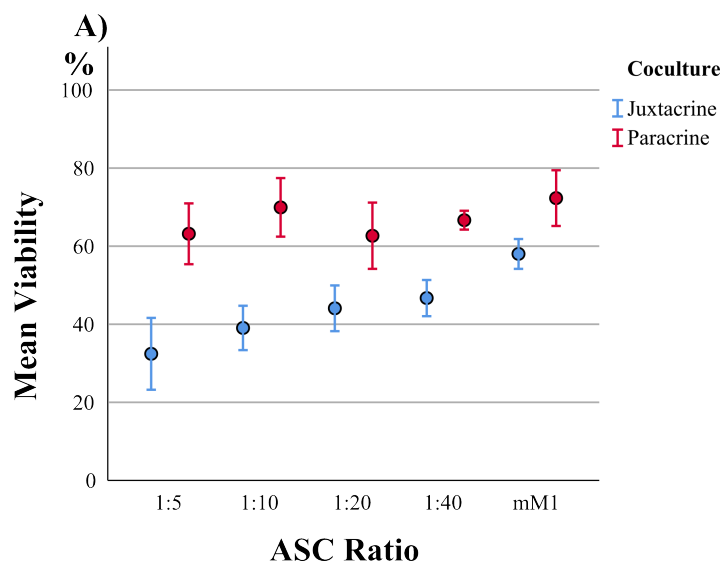
The viability of the macrophages in the juxtacrine co-culture was lower compared to paracrine

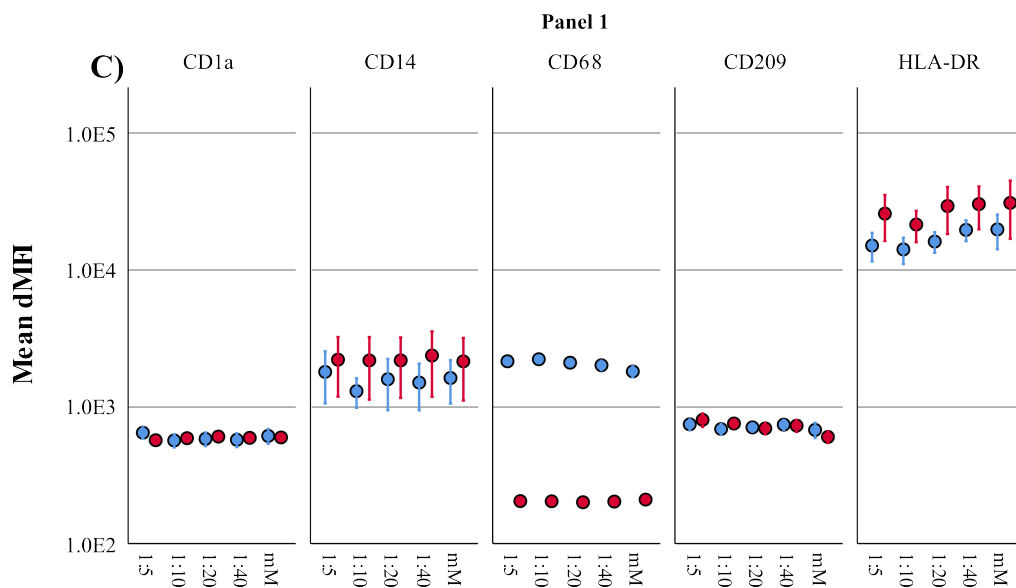
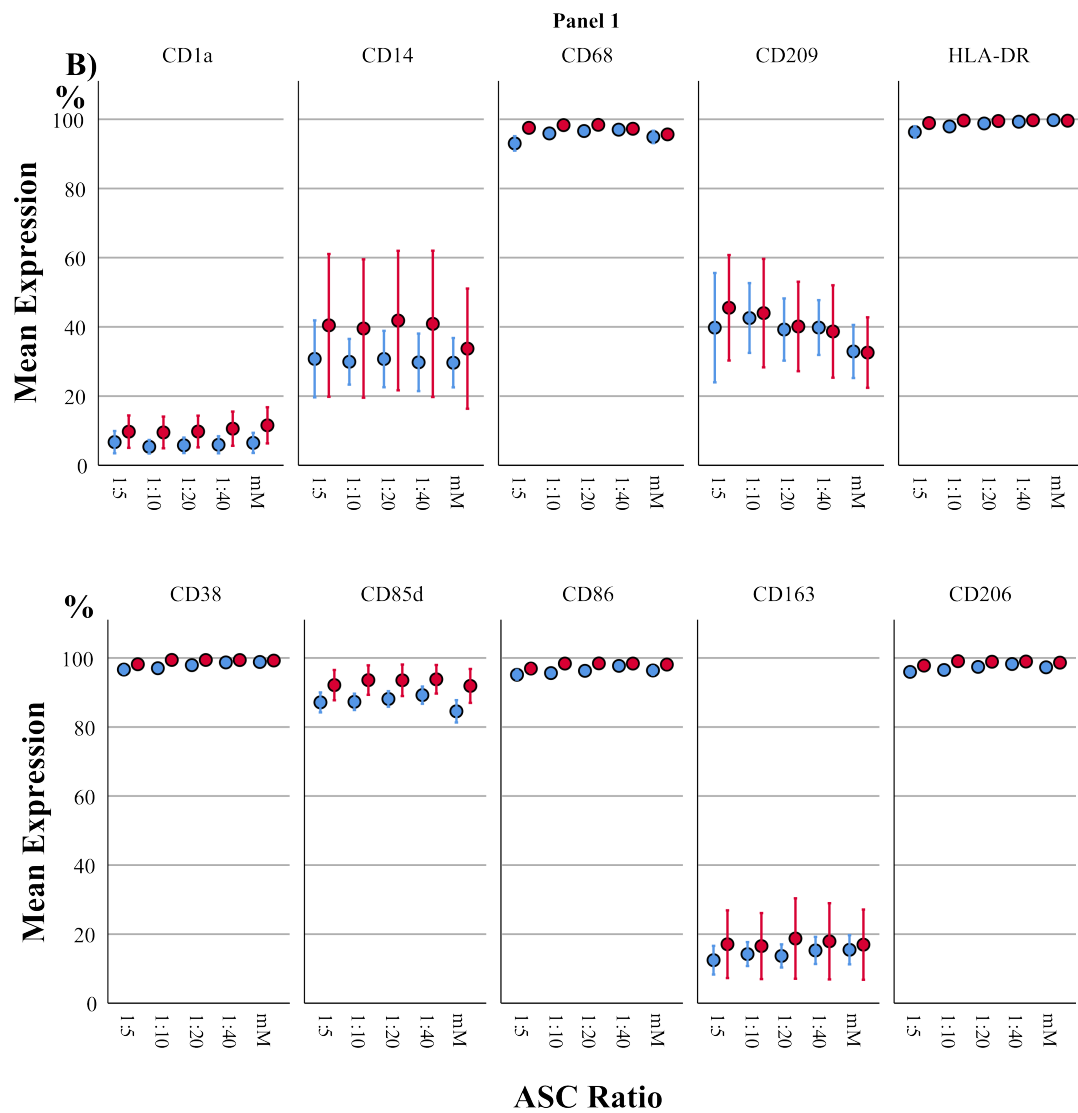
co-culture. Additionally, in the juxtacrine co-culture the viability decreased with increasing ratio of AT-MSC compared to the control (mature M1 phenotype), henceforth referred to as mM1 control (figure 3.8A).

The cells were negative for CD1a and CD163 and highly positive for CD38, CD68, CD86, CD206 and HLA-DR in both co-cultures at all ratios. The number of cells expressing CD14 and CD85d were increased in the paracrine co-culture compared to mM1 and juxtacrine co-culture. Additionally, both co-cultures resulted in an increased number of cells expressing CD209 at increasing ratio of AT-MSC (figure 3.8B). These results were supported by data for dMFI. Furthermore, the expression level of CD206 was highest at a ratio of 1:5, while CD38 was lowest at this ratio. The expression level of CD86 and HLA-DR were lowest at 1:10 in both co-cultures (figure 3.8C).

The secretion of IL-12p70 and TNF- α was lowest when the M1 macrophages had been cultured with AT-MSC at a ratio at 1:5 (3.8D), except from secretion of IL-12p70 in the paracrine co-culture, where the secretion was lowest at a ratio at 1:40. Additionally, the mM1 macrophages secreted the highest amount of IL-12p70 and TNF- α compared to both co-cultures, except from secretion of IL-12p70 in the juxtacrine co-culture, where the secretion was highest at a ratio of 1:20.

Based on the presented results, the optimal ratio of AT-MSC and macrophages is 1:5 argued by the low viability, lower expression of the pro-inflammatory markers CD38, CD86 and HLA-DR, increased expression of CD14 and CD206 and lowest secretion of IL-12p70 and TNF- α .





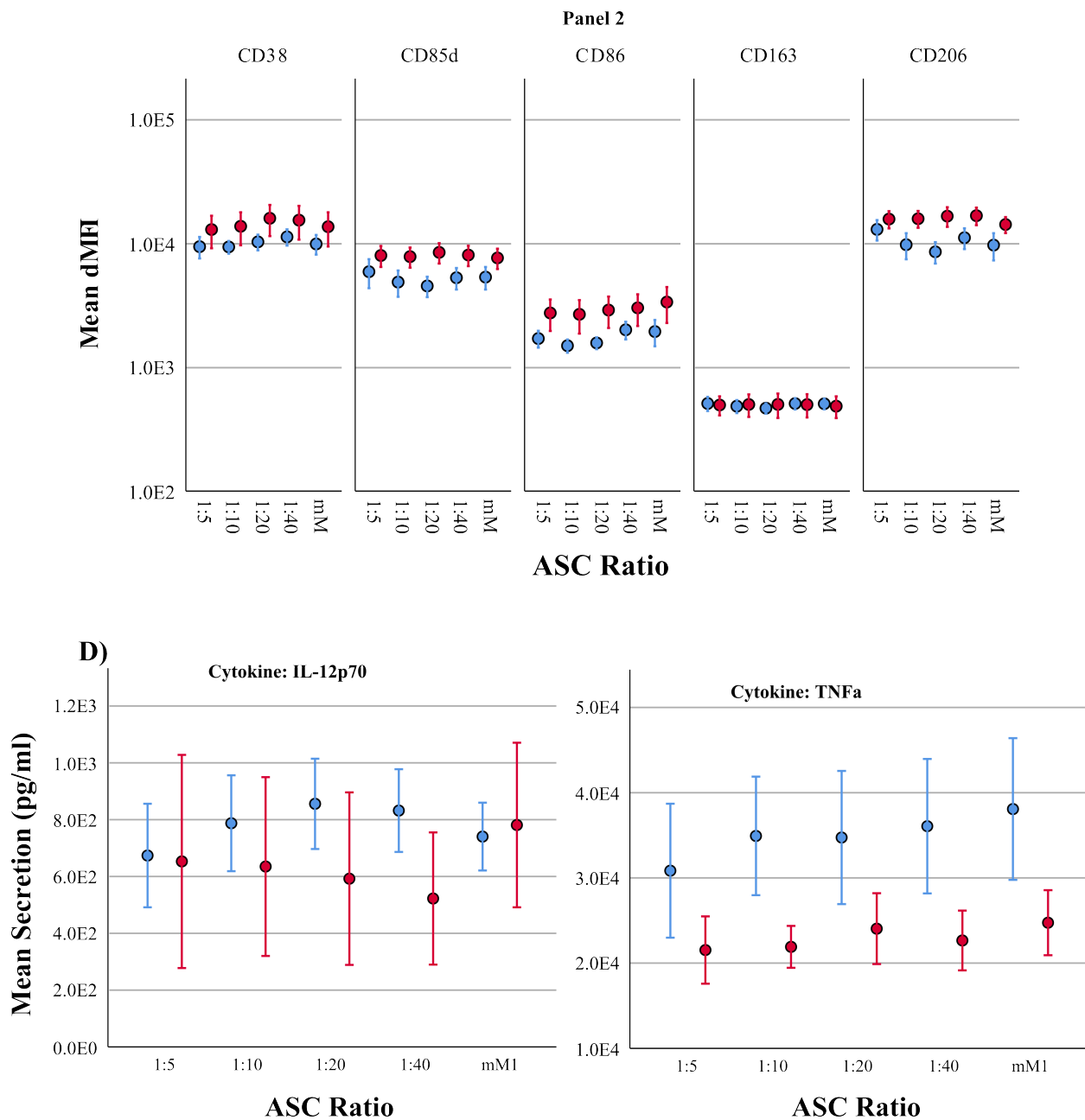


Figure 3.8: Note: ASC ratio is an abbreviation for AT-MSC ratio. **A)** Viability of M1 macrophages co-cultured with AT-MSC at different ratios (1:5, 1:10, 1:20 or 1:40 (AT-MSC:M1), in a juxtacrine (blue) or paracrine system (red). **B)** Portion of M1 macrophages which positively or negatively expressed a marker of Panel 1 and Panel 2 at different ratios of AT-MSC. **C)** Mean dMFI of each marker in Panel 1 and Panel 2 expressed on M1 macrophages when co-cultured with AT-MSC at different ratios in either a juxtacrine or paracrine system. **D)** Mean secretion of IL-12p and TNF- α secreted by M1 macrophages when co-cultured with AT-MSC at different ratios in either a juxtacrine or paracrine system. The mature phenotype (mM1) was applied as a control. dMFI: delta Median Fluorescence Intensity. Juxtacrine: n= 7, Paracrine: n= 3, \pm 1 SE

3.6 Phagocytosis

The phagocytotic properties of macrophages were investigated by exposing the cells to beads. Initially, the optimal concentration of beads was determined on immature M1 macrophages by titration in a 3-folds dilution ranging from 8.1×10^7 beads/ml to 1×10^6 (equal to 81 to 1 beads/cell).

3.6.1 Bead Concentration and Exposure Time

The number of phagocytised beads was affected by bead concentration and time of exposure (figure 3.9). Due to the technical challenges in distinguishing between macrophages having ingested more than six beads (described in the method section 2.7), the optimal concentration was determined to be 1×10^7 beads/ml (equal to 10 beads/cell). At this concentration the phagocytotic properties of the macrophages were clearly demonstrated; a considerable number of cells were actively phagocytising and few had engulfed excessive bead counts.

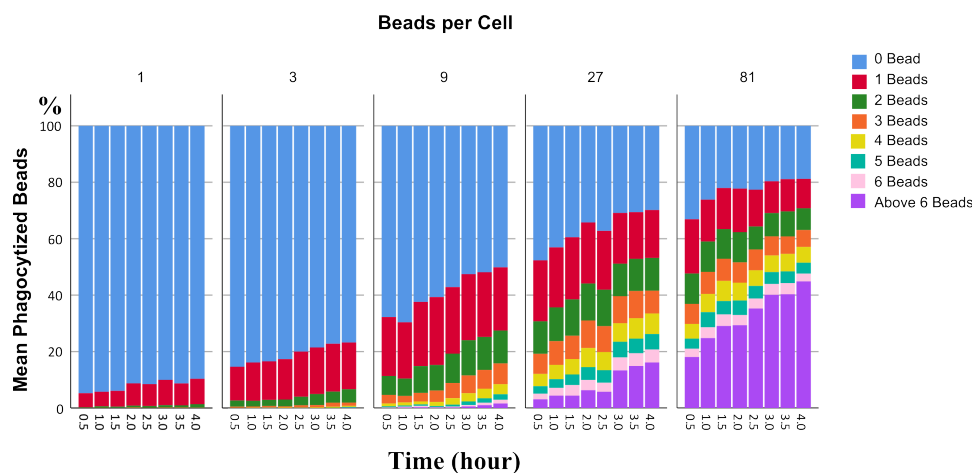


Figure 3.9: The percentage of phagocytising immature M1 macrophages and the percentage of how many of the macrophages which had phagocytised one bead, two beads etc. at different time points (0.5, 1, 1.5, 2, 2.5, 3, 3.5 and 4 hours), when exposed to beads at different concentrations (1, 3, 9, 27 and 81 beads/cell). n=2

However, at a concentration of 1×10^7 beads/ml, the total number of phagocytising cells might still be increasing. To investigate and determine the ideal time frame, the assay duration was tested on different phenotypes. Samples were analysed after 0, 2, 16, 20, and 24 hours.

The phagocytotic activity was highest until 16 hours from where immature M1 and M2 macrophages reach a plateau, and the mature phenotypes maintain the phagocytotic activity, however to a lesser extent (figure 3.10A). Despite reaching an apparent saturation in the number of phagocytising cells,

the macrophages continued to phagocytise beads leading to an increased percentage of macrophages which had phagocytised more than 6 beads (3.10B). Based on these results, the optimal exposure time of macrophages for the beads was 16 hours.

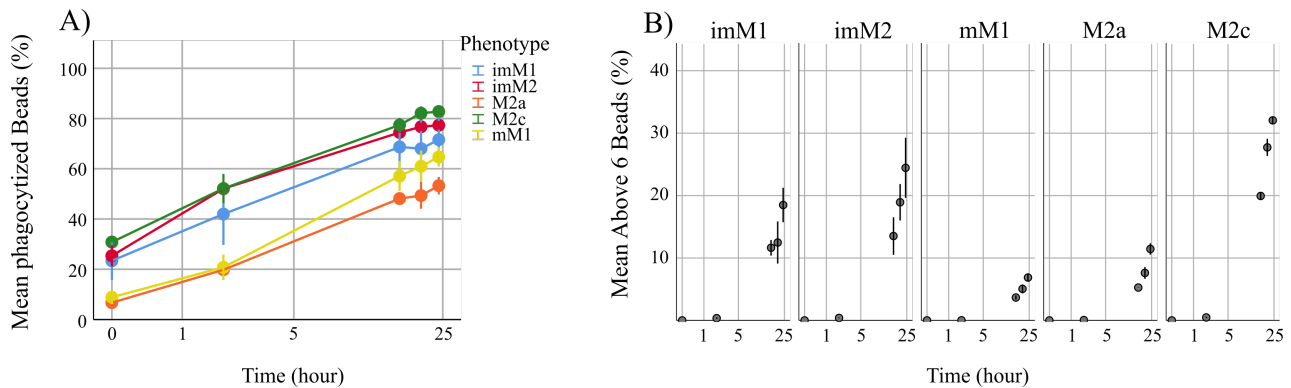


Figure 3.10: **A)** Percentage of phagocytising cells for each generated phenotype (immature M1, M2, mature M1, M2a and M2c macrophages), which had phagocytised at least one bead over time. **B)** Percentage of each phenotype which had phagocytised more than 6 beads over time (0, 2, 16, 20 and 24 hours).

To ensure the macrophages had indeed phagocytised the beads, microscopy was applied to demonstrate that the beads were located inside the cells (figure 3.11).

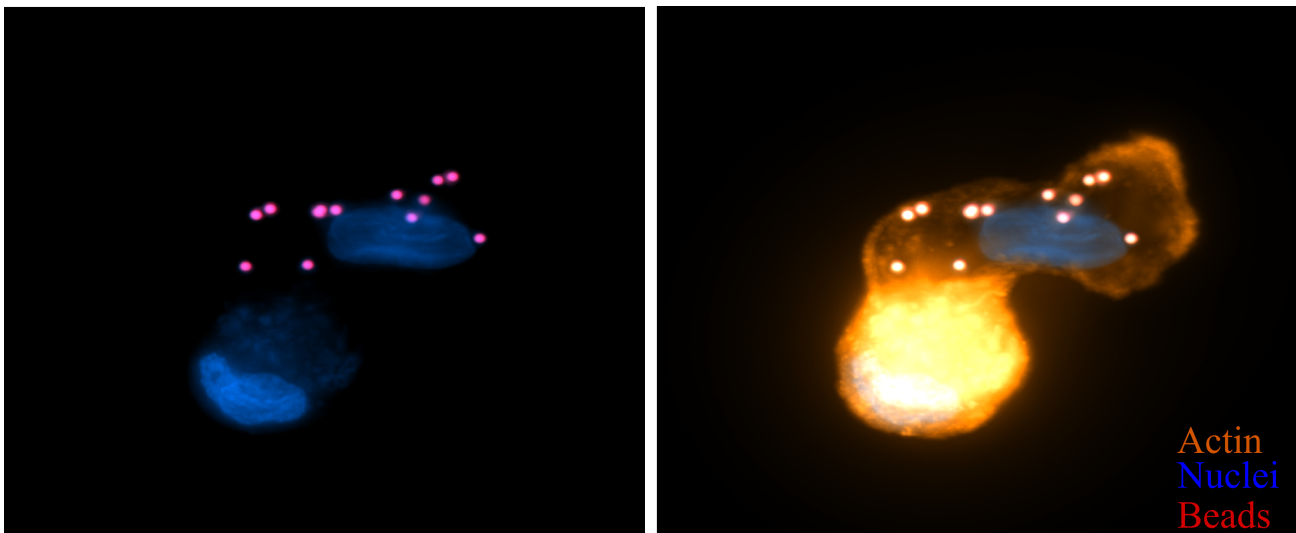


Figure 3.11: Two macrophages exposed to beads. One of the macrophages, bottom to the left, had not phagocytised any beads, but the other one had phagocytised 12 beads - all beads were validated to be inside the cell. These represent the extreme outcomes of the assay. The blue colour represents nuclei stained with DAPI, the orange represents actin filaments stained with stained with phalloidin, and the red represents the beads.

3.7 Co-culture with AT-MSC and Macrophages

The immunomodulatory properties of AT-MSC on M1, M2a and M2c macrophages were investigated on the established macrophage protocol.

The addition of AT-MSC to the mature phenotypes reduced the viability of the three subtypes of macrophages, when the cells were co-cultured in a juxtacrine system compared to the paracrine co-culture and the mature phenotype. The greatest impact on the viability was observed for M1 macrophages (figure 3.12).

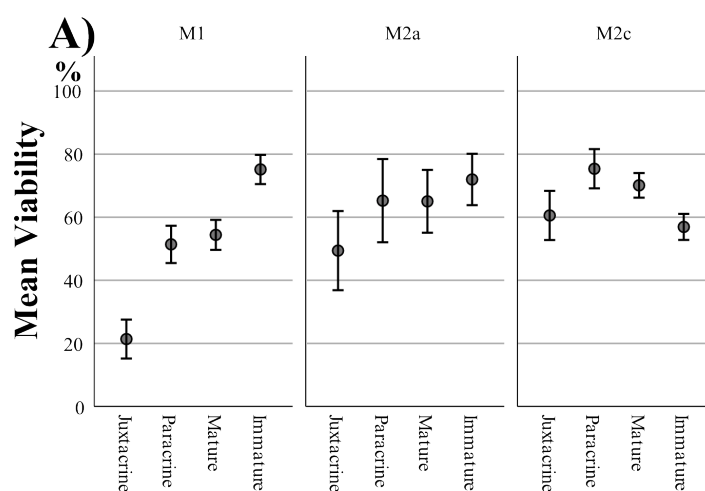


Figure 3.12: Viability of the three subtypes of macrophages at different conditions including juxtacrine and paracrine co-culture with AT-MSC, activated (mature) and unactivated (immature).

3.7.1 Effect of AT-MSC on marker expression on M1 macrophages

The co-cultured M1 macrophages in both co-cultures were highly positive for CD68, HLA-DR, CD38, CD85d, CD86 and CD206, while the number of cells expressing CD1a, CD163 and CD209 were low. However, the AT-MSC enhanced the number of cells positive for CD14, CD85d and CD209 in both co-cultures compared to the mature phenotype (figure 3.13A), while only the juxtacrine co-culture increased the number of cells expressing CD68. The expression of this marker was significantly higher on M1 macrophages in the juxtacrine co-culture compared with the mature M1 ($p=0.003$). A trend for the opposite was observed for the expression of CD38, CD86 and HLA-DR in the juxtacrine co-culture, however, the difference was not statistical significant (figure 3.13A and B). All together, these results indicated that AT-MSC in a juxtacrine co-culture had an impact on the maturation of M1 macrophages.

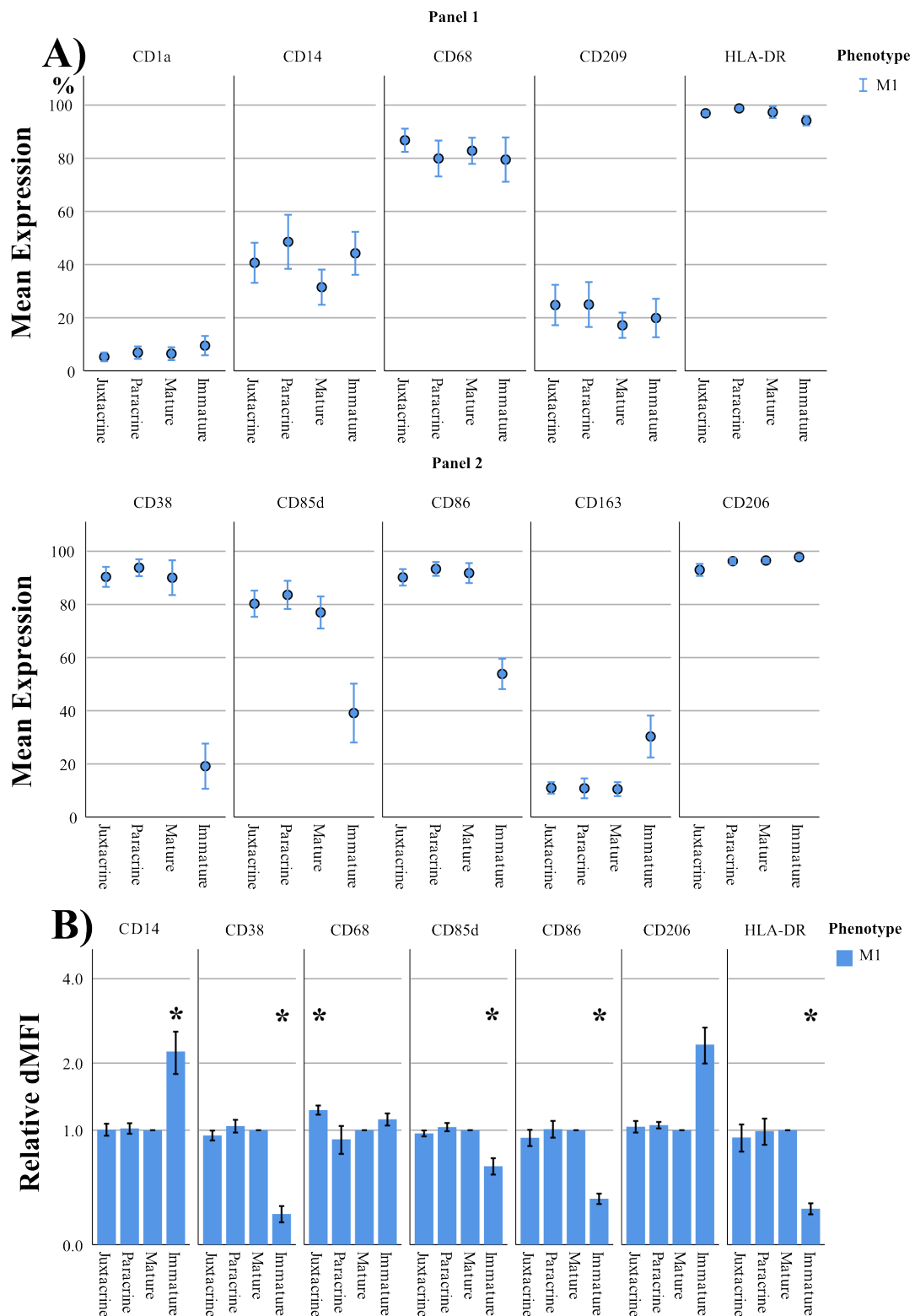
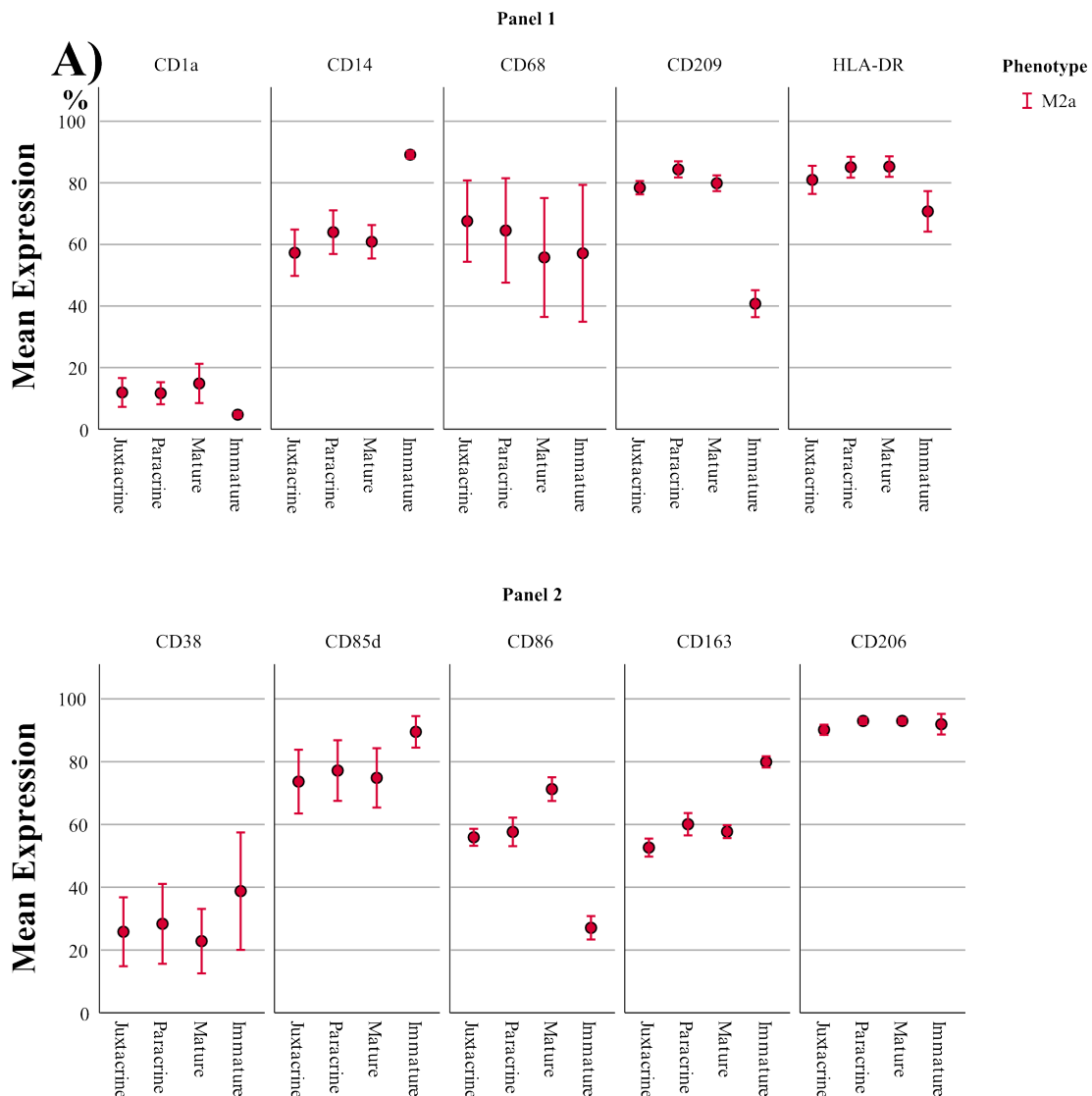


Figure 3.13: B) Normalised data of dMFI to the mature M1 macrophage. Only markers which expressed at least 25% of the mature macrophages were included in the statistical analysis of marker expression. * represents a statistical significant difference, at a significance level at 0.05%, to the mature M1 macrophages. Mature and juxtacrine: n=10, immature and paracrine: n=8, CD68: n=5 ± 1 SE, dMFI: delta Median Fluorescence Intensity, SE: Standard Error

3.7.2 Effect of AT-MSC on marker expression on M2a macrophages

The number of M2a macrophages expressing CD68 slightly increased when co-cultured with AT-MSC. The number of M2a macrophages expressing CD86 decreased (figure 3.14A) in both co-cultures, while HLA-DR only decreased in the juxtacrine co-culture. The expression level of CD86 and HLA-DR were significantly different between the juxtacrine co-culture and the mature phenotype ($p=0.003$ $p=0.006$, respectively), (figure 3.14B). Furthermore, M2a macrophages co-cultured with AT-MSC in both co-cultures increased the expression of CD14, CD85d, CD163 (except from juxtacrine co-culture), CD206 and CD209, to the same or higher level compared to the mature M2a macrophages (figure 3.14B).

These results indicated that AT-MSC impact the maturation of M2a macrophages.



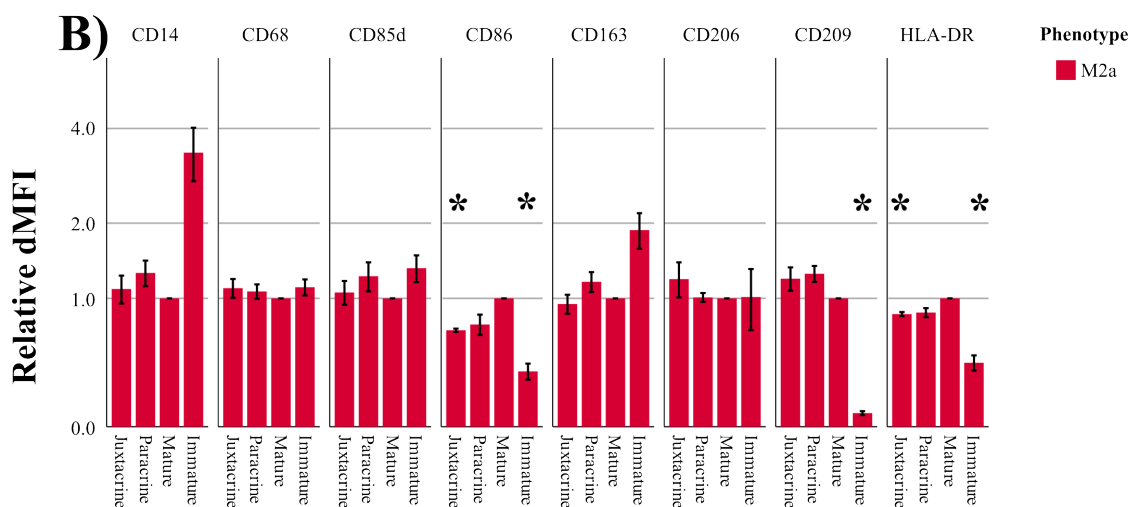


Figure 3.14: B) Normalised data of dMFI to the mature M2a macrophage. Only markers which expressed at least 25% of the mature macrophages were included in the statistical analysis of marker expression. All conditions were compared to the mature phenotype. * represents a statistical significant difference, at a significance level at 0.05%, to the mature M2a macrophages. n=4, ± 1 SE dMFI: delta Median Fluorescence Intensity, SE

3.7.3 Effect of AT-MSC on marker expression on M2c macrophages

The number of M2c macrophages expressing CD68, CD209, CD85d, CD163 and CD206 was lowest, when the cells had been co-cultured with AT-MSC in a juxtacrine co-culture, while the number of cells expressing HLA-DR was lowest in the paracrine co-culture compared to the mature M2c macrophages (figure 3.15A and B). Additionally, the paracrine co-culture resulted in increased expression level of CD38 on M2c macrophages compared to the mature phenotype. These results indicated that the AT-MSC impact the marker expression on M2c macrophages, in both types of co-culture and thereby might impact the maturation.

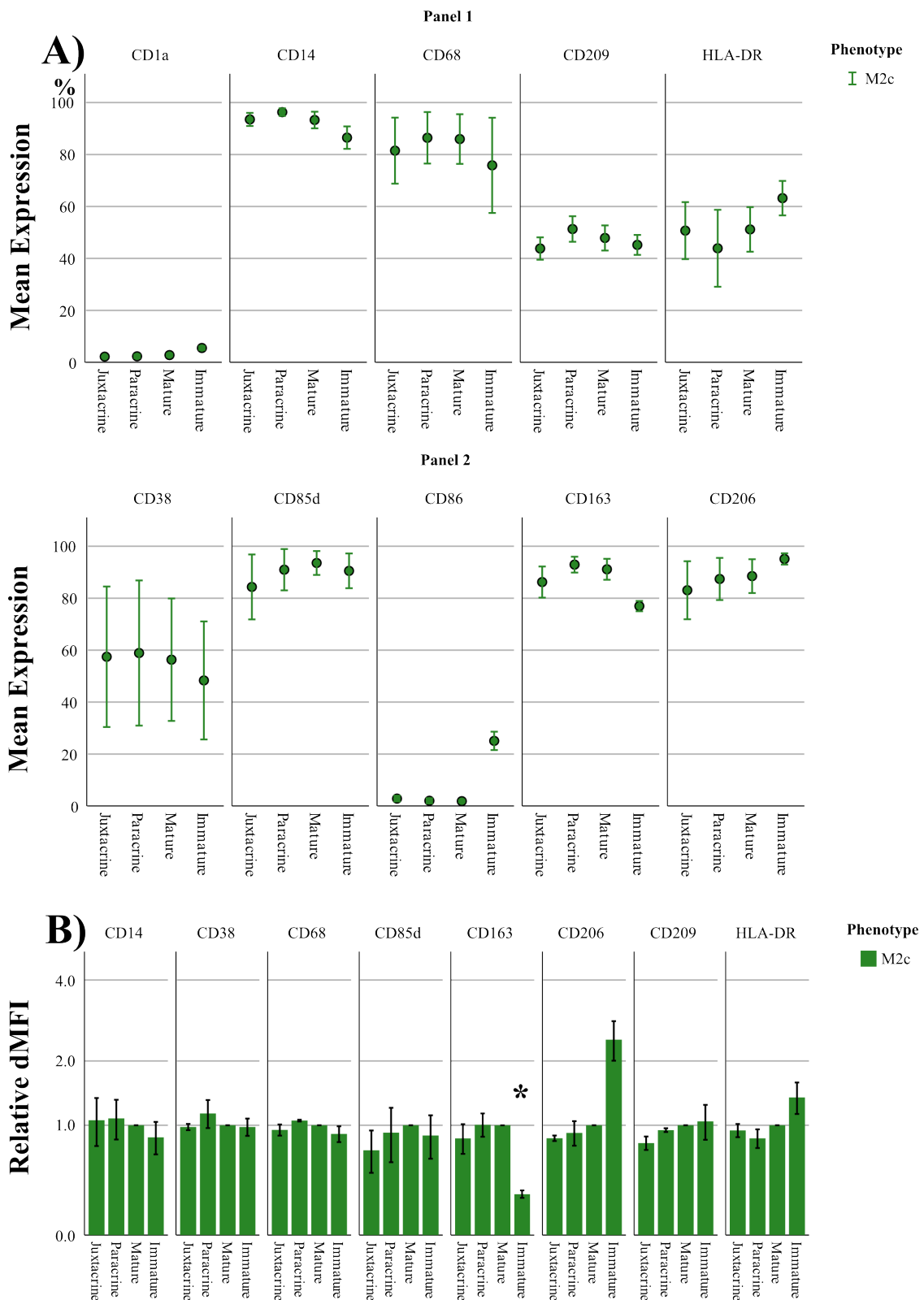


Figure 3.15: Normalised data of dMFI to the mature M2c macrophage. Only markers which were expressed at least 25% of the mature macrophages were included in the statistical analysis of marker expression. * represents a statistical significant difference, at a significance level at 0.05%, to the mature M2c macrophages. n=3, ± 1 SE dMFI: delta Median Fluorescence Intensity, SE

3.7.4 Mixed Lymphocyte Reaction

The highest proliferative response of allogeneic lymphocytes was elicited by mature M1 macrophages, which was more than twice the extent of M2a and M2c macrophages on Dil/P and DI, and a more modest difference on RI and PF (figure 3.16). AT-MSC caused a decrease in the ability to induce proliferation of allogeneic lymphocytes by M1 macrophages, indicated by PF and Dil/P, which was significantly decreased when co-cultured with AT-MSC in a juxtacrine system ($p=0.036$, $p=0.048$, respectively). A similar pattern was observed for M2c macrophages, however, only PF was significantly decreased in juxtacrine and paracrine co-culture ($p=0.003$), while the proliferation increased when M2a macrophages were co-cultured with AT-MSC. Indicated by RI, the number of responder cells were significantly lower in the juxtacrine co-culture for M1 macrophages compared to the mature phenotype ($p=0.036$), the opposite was observed for M2a and M2c macrophages (figure 3.16). Additionally, as indicated by DI, the average number of divisions of cells in the culture were significantly decreased by M1 macrophages co-cultured in a juxtacrine system and M2c macrophages co-cultured in both system compared to their mature phenotype (M1: $p=0.036$, M2c p 's= 0.003), while the opposite was observed for M2a macrophages.

These results indicated that AT-MSC impact the ability of M1 and M2c macrophages to induce proliferation of allogeneic lymphocytes. This was particularly apparent for M1 macrophages co-cultured in a juxtacrine system. Additionally, M2a and M2c macrophages induce proliferation to a lesser extent compared to the M1 macrophages. However, it was indicated that AT-MSC promote the ability of M2a macrophages to induce the proliferation.

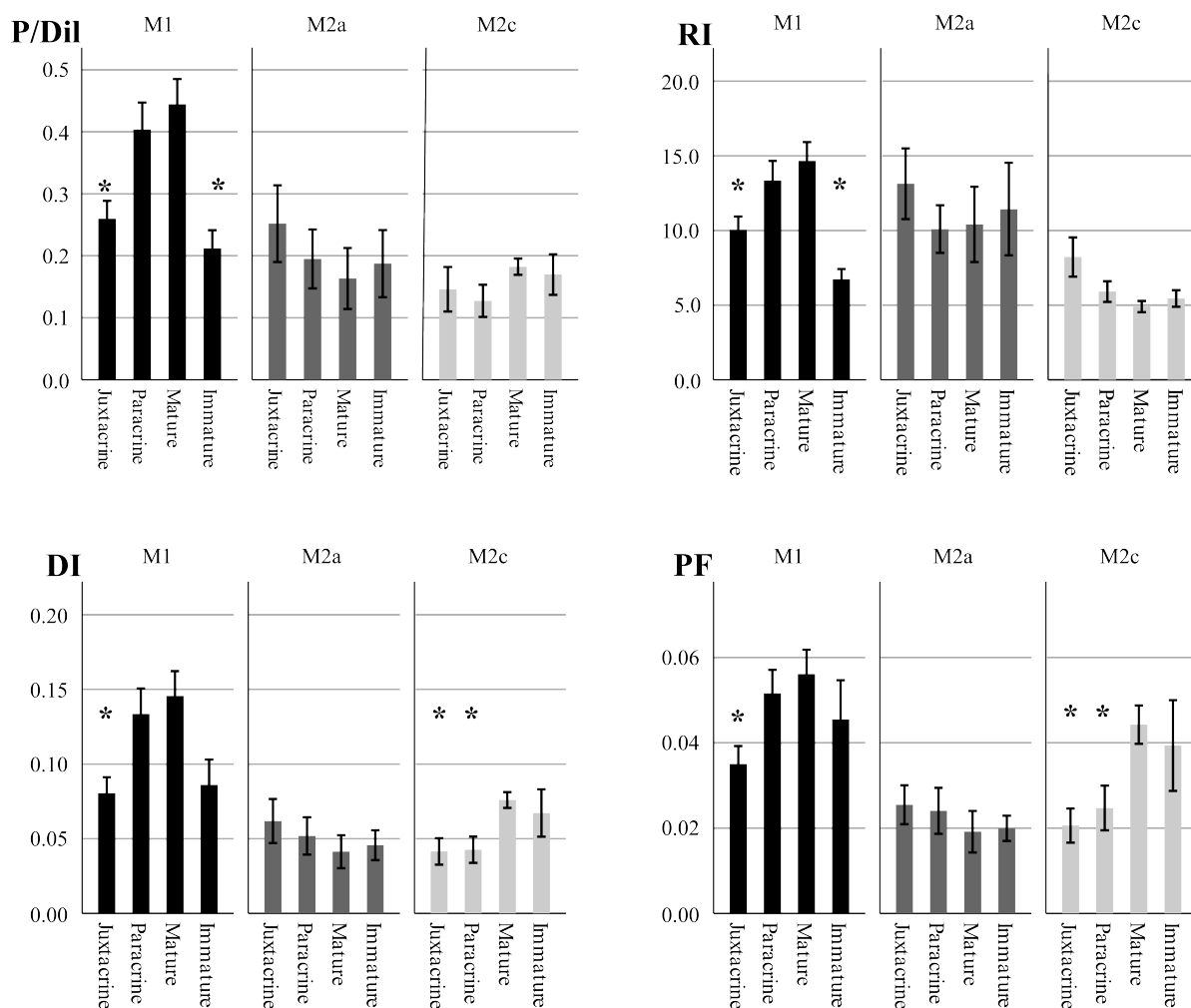


Figure 3.16: Analysis of the five generated macrophages (immature M1 and M2, mature M1, M2a and M2c) ability to induce proliferation of allogeneic lymphocytes. Additionally, the impact of AT-MSC on the macrophages ability to induce proliferation is illustrated. * represents a statistical significant difference, at a significance level at 0.05%, to the mature phenotype. Dil/P: Fraction Diluted, RI: Replication Index, DI: Division Index, PF: Precursor Frequency M1: n=12 (juxtacrine n=8), M2a: n=4, M2c: n=4

3.7.5 AT-MSC Impact on the Phagocytotic Properties of Macrophages

M2c macrophages had higher phagocytotic capacity compared to M1 and M2a macrophages which was increased by co-culture with AT-MSC, while the percentage of phagocytising M1 and M2a macrophages in juxtacrine co-culture decreased. This trend was most notable for M1 macrophages, though there was only a single observation for this condition (figure 3.17A). These findings were supported by average bead uptake per cell (figure 3.17C). However, AT-MSC did not decrease the number of beads phagocytised by the "active" phagocytising M1 and M2a macrophages. Furthermore, it was shown that M2c macrophages in a juxtacrine co-culture approximately had phagocytised one more

bead compared to the mature phenotype (figure 3.17B).

By microscopy it was validated that beads were inside the cells. Additionally, microscopy of the AT-MSC treated macrophages and the controls (immature and mature phenotypes) confirmed the phagocytotic capacity (figure 3.18), as previously described.

These results indicate that AT-MSC does not impact "active" phagocytising cells, meaning that these cells did not phagocytise more beads, except from M2c macrophages in a juxtacrine co-culture. However, the AT-MSC impact the number of "active" phagocytising cells.

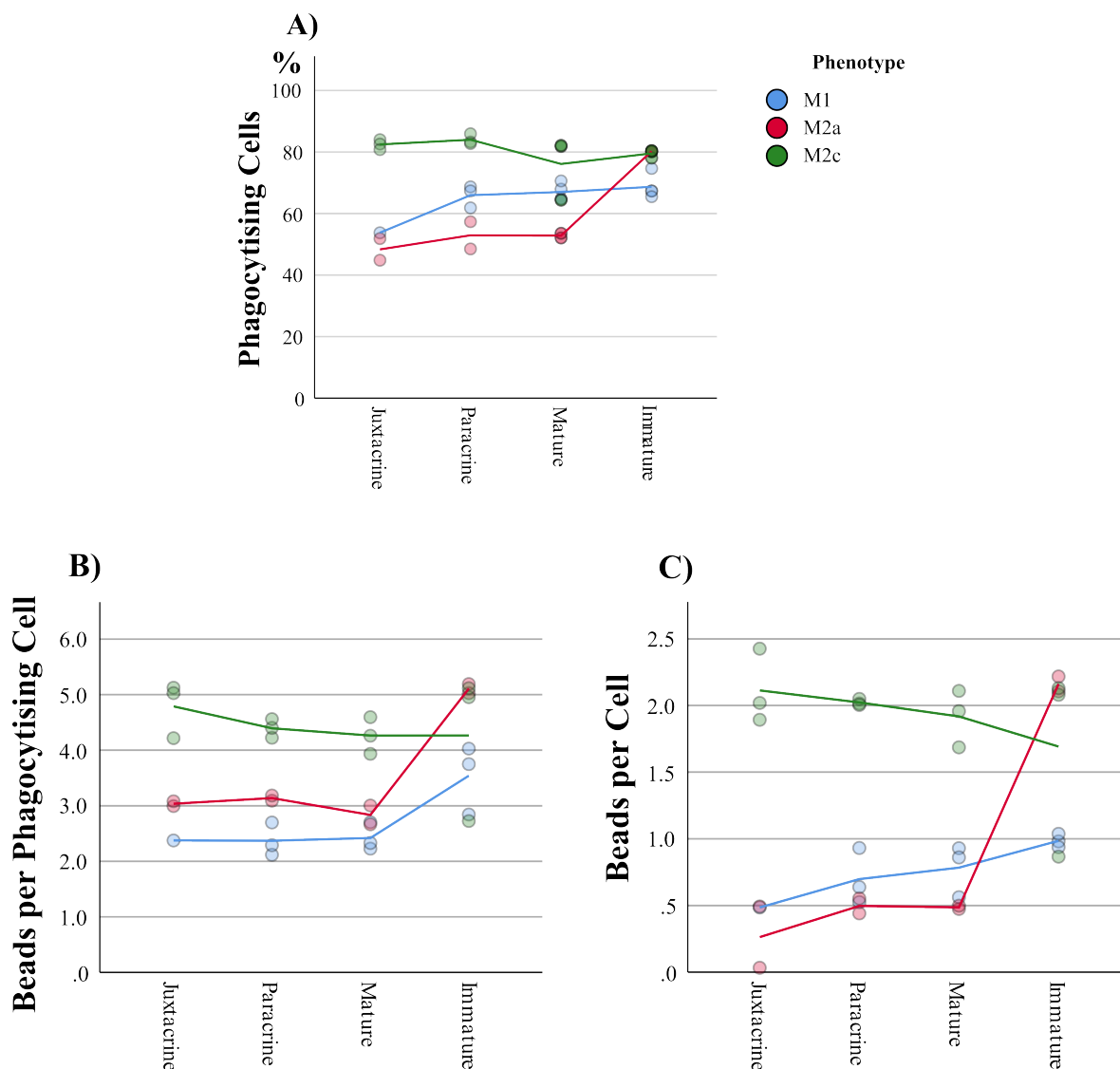


Figure 3.17: **A)** Mean percentage of phagocytising cells of each phenotype. **B)** Average number of phagocytised beads by the phagocytising phenotypes. **C)** Average number of phagocytised beads for the whole population of each phenotype. M1: n=3, except for the juxtacrine co-culture (n=1), M2a: n=2, M2c: n=3

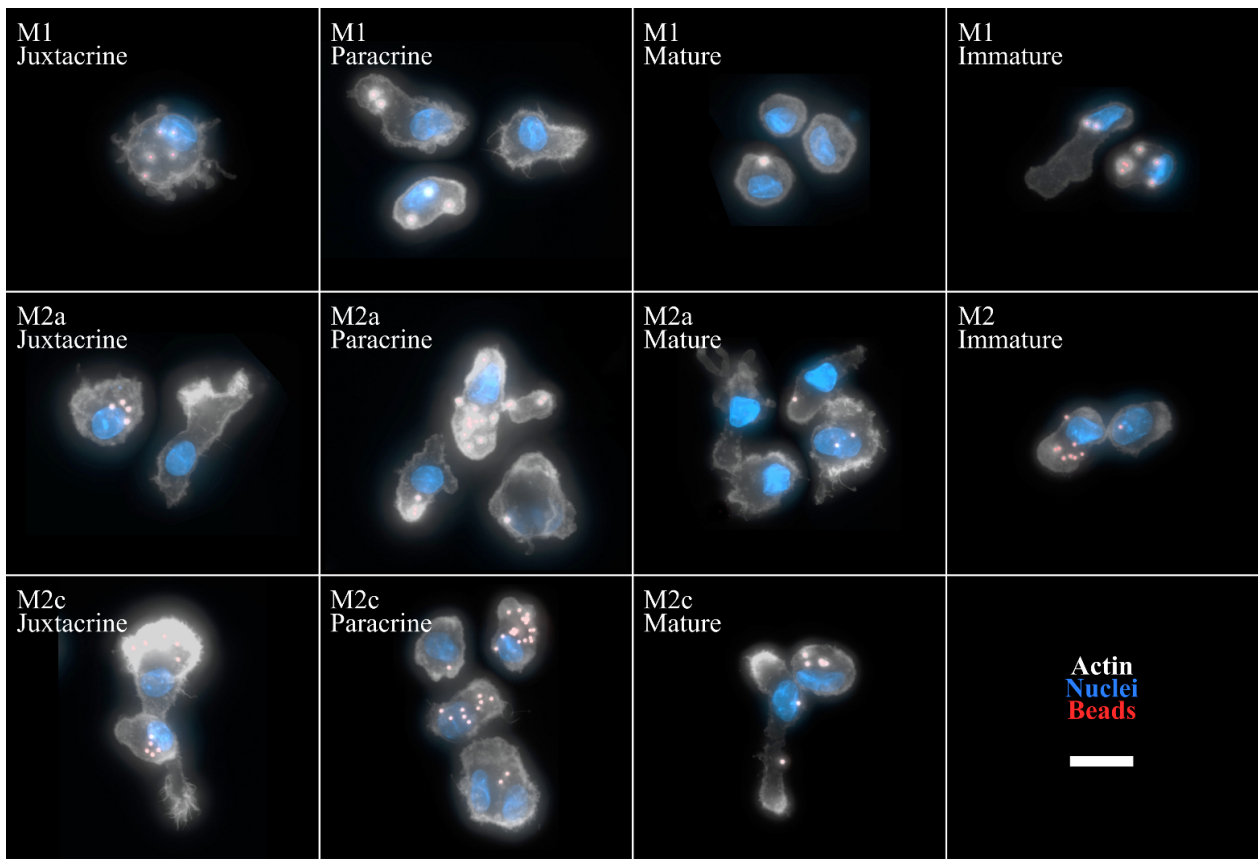


Figure 3.18: Phagocytotic capacity of the three different mature phenotypes (M1, M2a and M2c), the impact of AT-MSC on the mentioned phenotypes when co-cultured in either a juxtacrine or paracrine system and the phagocytotic capacity of immature macrophages. The nuclei were stained with DAPI, represented in blue, the actin filaments were stained with phalloidin, represented in white, the beads was loaded with crimson, represented in red.

4 Discussion

In this study, we generated distinct phenotypes of macrophages: two immature and three mature phenotypes. We found that immature monocyte-derived M1 macrophages could be generated by addition GM-CSF. The concentration of GM-CSF, did not affect the level of marker expression, indicating a robust immature M1 phenotype (figure 3.1). Additionally, we found that this phenotype was characterised as CD14⁺, CD68⁺ and HLA-DR⁺ in agreement with other studies [28, 30, 31]. Contrarily, we found that the generation of immature anti-inflammatory M2 macrophages were dependent on the concentration of M-CSF, since low concentration of M-CSF resulted in high degree of cell death (figure 3.1). Even though the immature M1 and M2 macrophages share markers, expression of other markers allows for discrimination. We showed that immature M1 macrophages do not express CD209 whereas immature M2 macrophages are positive for this marker. CD209 has been reported as a DC marker [43] (a phenotypical profile of DC is available in appendix 5.4), however, M2 macrophages also express this marker, which may be explained by the fact that M-CSF induces expression of CD209 [45]. Additionally, we showed that the immature M2 macrophages have higher expression of CD14 but lower expression of CD206 compared to the immature M1 phenotype, in accordance with other studies [29, 29, 46].

We showed that activation of macrophages lead to generation of distinct phenotypes with altered morphology, marker expression and functionality, which occurs in response to multiple types of activating factors or stimuli (figures 3.6, 3.7, 3.10 and 3.16). M1 macrophages activated with LPS alone express higher levels of CD14 compared to the M1 macrophages activated with LPS in combination with IFN- γ (figure 3.3 and 3.4). By these data it was indicated that IFN- γ decreased the expression CD14. However, CD14 is involved in transferring LPS to TLR-4 [47] and might be the explanation of the increased expression when activated with LPS alone. Additionally, the secretion of IL-12p70 was undetectable when activated with LPS alone and detectable with the addition of IFN- γ (figure 3.4D). These findings indicated that the combination of LPS and IFN- γ leads to a more mature pro-inflammatory M1 macrophage.

On the other hand, different anti-inflammatory subtypes derived from immature M2 macrophages can be generated by addition of cytokine(s). We showed that the M2a macrophages had lower expression of CD14 and higher expression of CD206 compared to the M2c macrophages, which were highly positive for CD14, CD85d and CD163 (figure 3.5). These findings were in agreement with other stud-

ies which have suggested that M2a macrophages are characterised as CD14⁻ and CD206⁺ [34] and M2c characterised as CD14⁺ CD163⁺ [34, 35]. Several studies have activated M2a macrophages with IL-4 in combination with IL-13 [24, 48, 49]. Our data indicate, in agreement with other studies [11, 35], that for M2a the phenotypic profile is independent of IL-13, however, the functionality of the cells can possibly be altered with the combination of both cytokines.

The phagocytotic capacity varied depending on the phenotype (figure 3.10). We demonstrated that the immature M2 macrophages had a slightly higher phagocytotic capacity compared to the immature M1 macrophage. This is in agreement with Xu et al. [29]. Additionally, we showed that M2c macrophages phagocytised more than other phenotypes. This may be due to the activating stimuli as it is suggested that IL-10 increases the phagocytotic capacity in agreement with Zizzo et al. [25] but not reported by Xu et al. [29]. Both studies agreed that immature M2 macrophages and IL-10 activated (M2c) macrophages prefer to phagocytise apoptotic cells, a process known as efferocytosis [50]. We observed a high degree of cell death in cultures of immature M2 in presence of low concentration of M-CSF (figure 3.1A) and in juxtacrine co-culture of M1 macrophages (figure 3.12A). Additionally, it was observed that the expression of CD68 was increased on remaining viable cells in these conditions, indicating that efferocytosis is associated with increased expression of CD68. This correlation could be explained by the fact that CD68 is a protein present on lysosomes [51] and that Phosphatidylserine, expressed on apoptotic cells, is ligand for CD68 [52, 52–55]. Furthermore, it is indicated by our findings and other studies that there is a correlation between increasing phagocytotic uptake and increased expression of CD163 and CD14 [25, 29]. This manifestation might be apparent in phagocytosis of other substances, which possibly can explain the distribution of the phagocytotic phenotypes of macrophages observed in this study (figure 3.10). The phagocytotic capacity of each phenotype might be enhanced by opsonisation to target the phenotype of interest [25, 29, 56]. Further experiments are needed for investigations of opsonisation of beads to target phenotypes.

In this thesis, it is hypothesised that AT-MSC impact the maturation of the M1 mature phenotype resulting in a less pro-inflammatory phenotype. Additionally, immunomodulatory properties of AT-MSC were investigated on M2a and M2c macrophages, but the interaction of AT-MSC with M1 macrophages was the primarily focus.

We showed that M1 macrophages co-cultured with AT-MSC in a juxtacrine co-culture decreased the expression of CD38, CD86 and HLA-DR, compared to the untreated mature phenotype (figure 3.13B). These findings indicate that AT-MSC had immunomodulatory effects on maturation of macrophages, leading to a less pro-inflammatory M1 phenotype, while AT-MSC result in a more anti-inflammatory phenotype for M2a and M2c macrophages. The mechanisms that might be responsible for the immunomodulatory effects of MSC was beyond the current scope and will therefore not be discussed in this report.

The decreased expression of CD86 is in agreement with Ambuaree et al. [11], which co-cultured CD14⁺ monocytes from day 0, in polarisation medium (GM-CSF), with MSC-derived from placenta (P-MSC) in a juxtacrine and paracrine co-culture in a lower ratio of P-MSC. Additionally, they found increased expression of HLA-DR in both conditions. They suggest that P-MSC added during differentiation could alter the differentiated M1 macrophage phenotype to a *M2-like phenotype*, described as high expression of CD14, CD163 and CD206.

Manferdini et al. [17], which co-cultured IFN γ activated M1 macrophages in a juxtacrine and paracrine system with AT-MSC (ratio at 1:1) for two days, showed that both co-cultures increased the level of CD163, whereas the level of CD206 was only increased in the paracrine co-culture compared to the mature phenotype. The findings of CD163 were measured by real time qRT-PCR and ELISA, which might explain the contradicting findings observed in this study. However, we found that CD206 was slightly increased in M1 macrophages co-cultured with AT-MSC. Furthermore, they investigated the effect of AT-MSC on immature M2 macrophages and reported no significant effect of the AT-MSC. However, their data showed decreased secretion of TNF- α in the juxtacrine culture and increased secretion of IL-10 in paracrine co-culture, indicating that AT-MSC have the ability to kind of boost the anti-inflammatory phenotypes. Additionally, these studies indicated that juxtacrine co-culture was not required for inducing the switch from M1 to M2 macrophage [17, 36], contradicting our results. Another study showed that BM-MSC co-cultured with M1 macrophages in a paracrine system at day 9 (ratio at 1:1), activated with LPS, led to an increase expression of CD206 and thereby suggested that M1 macrophages had switched to M2 macrophages, as they claimed that immature M1 macrophages had low expression of CD206 [36]. This is in contrast to the findings in this study and others [29]. A possible explanation to the low expression of CD206 may arise from the differentia-

tion protocol, which used GM-CSF at a concentration of 5 ng/ml, which might have been too low. Monocytes express low levels of CD206 (figure 5.1 in appendix), and it is difficult not to question whether the reported cells, which were solely defined based on CD206 and secretion of TNF α and IL-12, was indeed of a M1 phenotype. As positive control for the switch induced by MSC, they stimulated immature M1 macrophages with IL-4 and showed that the expression of CD206 was similar to MSC-treated M1 macrophages [36]. The comparison of MSC- and IL-4-treated M1 macrophages may be an oversimplification, as GM-CSF and IL-4 can result in generation of DC [46], which is positive for CD206 as well (appendix figure 5.4). This emphasises the need of implementation of a common standardised protocol for generation of macrophages *in vitro* to be utilised across research fields.

The percentage of phagocytotic M2a macrophages increased slightly when co-cultured with AT-MSC in a paracrine co-culture (figure 3.17), which might be related to upregulation of CD14 and CD163 (figure 3.14). Introduction of AT-MSC in co-culture with M1 macrophages did not affect phagocytosis, which correlates with the lacking upregulation of CD14 and CD163. However, it has been demonstrated by Ambuaree et al. that MSC are able to alter the phagocytotic capacity of macrophages, quantified by zymosan particles uptake [11].

Additionally, we found that AT-MSC in a juxtacrine co-culture suppressed the ability of M1 macrophages to induce proliferation of allogeneic lymphocytes. M2c macrophages, characterised by low expression of CD86 and HLA-DR, induced proliferation to a much lesser extent compared to the mature M1 and M2a macrophages, which was further reduced by treatment with AT-MSC (figure 3.16). It is possible that the reduced proliferation was associated with the downregulation of CD86 and HLA-DR induced by AT-MSC, since PMBC primarily consist of T-cells and CD86 and HLA-DR are important receptors for inducing the proliferation of these cells [57].

An important factor worth mentioning relates to the treatment of MSC. We applied AT-MSC, which were thawed immediately prior to co-culture with the macrophages. This might impair the immunomodulatory properties of the AT-MSC *in vitro* compared MSC cultured under more optimal conditions, that is, fully recovered after freezing/thawing and metabolically active, etc. However, we applied the AT-MSC to mimic the clinical cell-based product of CSCC as much as possible. This

is an important aspect for future experiments, because the purpose eventually is to use AT-MSC as treatment for diseases.

Due to the differences in the protocols for generation of macrophages, it is challenging to assess the properties of MSC on the macrophages as well as the capacity of the MSC to induce polarisation of a M1 macrophage into a M2a, M2b, M2c or maybe a fourth phenotype.

Conclusively, we demonstrated that the established protocol is applicable and valid for generation of different monocyte-derived macrophage phenotypes *in vitro*. Additionally, it is shown that AT-MSC have immunomodulatory properties and have the ability to switch mature M1 macrophages into a less pro-inflammatory phenotype with lower expression markers associated with inflammation and inhibited ability to induce proliferation of lymphocytes. Furthermore, it is reported that AT-MSC have the ability to boost anti-inflammatory phenotypes. Further investigation are needed to determine the mechanisms of action of AT-MSC to induce anti-inflammatory phenotypes of macrophages.

Bibliography

- [1] Arnold I Caplan. Mesenchymal stem cells. *Journal of Orthopaedic Research*, 9(5):641–650, 1991.
- [2] M Owen and A J Friedenstein. Stromal stem cells: marrow-derived osteogenic precursors. *Ciba Foundation symposium*, 136:42–60, 1988.
- [3] William C. Tavassoli, Mehdi and Crosby. Transplantation of Marrow to Extramedullary Sites. *Science*, 161(3836):54–56, 1968.
- [4] A J Friedenstein, R K Chailakhyan, and U V Gerasimov. Bone marrow osteogenic stem cells: in vitro cultivation and transplantation in diffusion chambers. *Cell and Tissue Kinetics*, 20(3):263–272, 1987.
- [5] Darwin J. Prockop, Daniel J. Kota, Nikolay Bazhanov, and Roxanne L. Reger. Evolving paradigms for repair of tissues by adult stem/progenitor cells (MSCs). *Journal of Cellular and Molecular Medicine*, 14(9):2190–2199, 2010.
- [6] Joni Ylöstalo, Nikolay Bazhanov, and Darwin J Prockop. Reversible commitment to differentiation by human multipotent stromal cells in single-cell-derived colonies. *Experimental hematology*, 36(10):1390–1402, 2008.
- [7] PubMed. Search of Mesenchymal Stem Cells. <https://pubmed.ncbi.nlm.nih.gov/?term=mesenchymal+stem+cells> Accessed from: <https://pubmed.ncbi.nlm.nih.gov/?term=mesenchymal+stem+cells>, 2021. Date accessed: 18/04 2021.
- [8] E M Horwitz, K Le Blanc, M Dominici, I Mueller, I Slaper-Cortenbach, F C Marini, R J Deans, D S Krause, and A Keating. Clarification of the nomenclature for MSC: The International Society for Cellular Therapy position statement. *Cytotherapy (Oxford)*, 7(5):393–395, 2005.
- [9] S Viswanathan, Y Shi, J Galipeau, M Krampera, K Leblanc, I Martin, J Nolte, D G Phinney, and L Sensebe. Mesenchymal stem versus stromal cells: International Society for Cell & Gene Therapy (ISCT®) Mesenchymal Stromal Cell committee position statement on nomenclature. *Cytotherapy (Oxford)*, 21(10):1019–1024, 2019.

BIBLIOGRAPHY

- [10] M. Dominici, K. Le Blanc, I. Mueller, I. Slaper-Cortenbach, F. C. Marini, D. S. Krause, R. J. Deans, A. Keating, D. J. Prockop, and E. M. Horwitz. Minimal criteria for defining multipotent mesenchymal stromal cells. The International Society for Cellular Therapy position statement. *Cytotherapy*, 8(4):315–317, 2006.
- [11] M. H. Abumaree, M. A. Al Jumah, B. Kalionis, D. Jawdat, A. Al Khaldi, F. M. Abomaray, A. S. Fatani, L. W. Chamley, and B. A. Knawy. Human Placental Mesenchymal Stem Cells (pMSCs) Play a Role as Immune Suppressive Cells by Shifting Macrophage Differentiation from Inflammatory M1 to Anti-inflammatory M2 Macrophages. *Stem Cell Reviews and Reports*, 9(5):620–641, 2013.
- [12] Mandana Haack-Sørensen, Bjarke Follin, Morten Juhl, Sonja K. Brorsen, Rebekka H. Søndergaard, Jens Kastrup, and Annette Ekblond. Culture expansion of adipose derived stromal cells. A closed automated Quantum Cell Expansion System compared with manual flask-based culture. *Journal of Translational Medicine*, 14(1):1–11, 2016.
- [13] Sarah A Wexler, Craig Donaldson, Patricia Denning-Kendall, Claire Rice, Ben Bradley, and Jill M Hows. Adult bone marrow is a rich source of human mesenchymal 'stem' cells but umbilical cord and mobilized adult blood are not. *British journal of haematology*, 121(2):368–374, 2003.
- [14] Samih Mohamed-Ahmed, Inge Fristad, Stein Atle Lie, Salwa Suliman, Kamal Mustafa, Hallvard Vindenes, and Shaza B Idris. Adipose-derived and bone marrow mesenchymal stem cells: a donor-matched comparison. *Stem Cell Research & Therapy*, 9(1):168, 2018.
- [15] Morten Juhl, Bjarke Follin, Monika Gad, Jesper Larsen, Jens Kastrup, and Annette Ekblond. Adipose Tissue-Derived Stromal Cells Induce a Highly Trophic Environment While Reducing Maturation of Monocyte-Derived Dendritic Cells. *Stem Cells International*, 2020:8868909, 2020.
- [16] Moira François, Raphaëlle Romieu-Mourez, Mengyang Li, and Jacques Galipeau. Human MSC suppression correlates with cytokine induction of indoleamine 2,3-dioxygenase and bystander M2 macrophage differentiation. *Molecular Therapy*, 20(1):187–195, 2012.

BIBLIOGRAPHY

- [17] C. Manferdini, F. Paoletta, E. Gabusi, L. Gambari, A. Piacentini, G. Filardo, S. Fleury-Cappellesso, A. Barbero, M. Murphy, and G. Lisignoli. Adipose stromal cells mediated switching of the pro-inflammatory profile of M1-like macrophages is facilitated by PGE2: in vitro evaluation. *Osteoarthritis and Cartilage*, 25(7):1161–1171, 2017.
- [18] Alfred I Tauber. Metchnikoff and the phagocytosis theory. *Nature Reviews Molecular Cell Biology*, 4(11):897–901, 2003.
- [19] R van Furth and Z A Cohn. The origin and kinetics of mononuclear phagocytes. *The Journal of Experimental Medicine*, 128(3):415–435, 1968.
- [20] Florent Ginhoux, Melanie Greter, Marylene Leboeuf, Sayan Nandi, Peter See, Solen Gokhan, Mark F Mehler, Simon J Conway, Lai Guan Ng, E Richard Stanley, Igor M Samokhvalov, and Miriam Merad. Fate mapping analysis reveals that adult microglia derive from primitive macrophages. *Science*, 330(6005):841–845, 2010.
- [21] Slava Epelman, Kory J Lavine, and Gwendalyn J Randolph. Origin and functions of tissue macrophages. *Immunity*, 41(1):21–35, jul 2014.
- [22] Aoife Kelly, Aleksander M Grabiec, and Mark A Travis. Culture of Human Monocyte-Derived Macrophages. *Methods Mol Biol*, 1784:1–11, 2018.
- [23] Michael Stein, Satish Keshav, Neil Harris, and Siamon Gordon. Interleukin 4 potently enhances murine macrophage mannose receptor activity: a marker of alternative immunologic macrophage activation. *The Journal of Experimental Medicine*, 176(1):287–292, 1992.
- [24] S. Mia, A. Warnecke, X. M. Zhang, V. Malmström, and R. A. Harris. An optimized protocol for human M2 macrophages using M-CSF and IL-4/IL-10/TGF- β yields a dominant immunosuppressive phenotype. *Scandinavian Journal of Immunology*, 79(5):305–314, 2014.
- [25] Gaetano Zizzo, Brendan A Hilliard, Marc Monestier, and Philip L Cohen. Efficient clearance of early apoptotic cells by human macrophages requires M2c polarization and MerTK induction. *Journal of immunology (Baltimore, Md. : 1950)*, 189(7):3508–3520, oct 2012.
- [26] Abbas Shapouri-Moghaddam, Saeed Mohammadian, Hossein Vazini, Mahdi Taghadosi, Seyed Alireza Esmaili, Fatemeh Mardani, Bitia Seifi, Asadollah Mohammadi, Jalil T. Afshari,

BIBLIOGRAPHY

- and Amirhossein Sahebkar. Macrophage plasticity, polarization, and function in health and disease. *Journal of Cellular Physiology*, 233(9):6425–6440, 2018.
- [27] Fernando Oneissi Martinez, Antonio Sica, Alberto Mantovani, and Massimo Locati. Macrophage activation and polarization. *Frontiers in bioscience*, 13(2):453–461, 2008.
- [28] Abdullah A. Tarique, Jayden Logan, Emma Thomas, Patrick G. Holt, Peter D. Sly, and Emmanuelle Fantino. Phenotypic, functional, and plasticity features of classical and alternatively activated human macrophages. *American Journal of Respiratory Cell and Molecular Biology*, 53(5):676–688, 2015.
- [29] Wei Xu, Anja Roos, Nicole Schlagwein, Andrea M Woltman, Mohamed R Daha, and Cees van Kooten. IL-10-producing macrophages preferentially clear early apoptotic cells. *Blood*, 107(12):4930–4937, 2006.
- [30] E Gottfried, L A Kunz-Schughart, A Weber, M Rehli, A Peuker, A Müller, M Kastenberger, G Brockhoff, R Andreesen, and M Kreutz. Expression of CD68 in non-myeloid cell types. *Scandinavian Journal of Immunology*, 67(5):453–463, 2008.
- [31] Anoop Babu Vasandan, Sowmya Jahnavi, Chandanala Shashank, Priya Prasad, Anujith Kumar, and S Jyothi Prasanna. Human Mesenchymal stem cells program macrophage plasticity by altering their metabolic status via a PGE(2)-dependent mechanism. *Scientific reports*, 6:38308, dec 2016.
- [32] Stephanie A Amici, Nicholas A Young, Janiret Narvaez-Miranda, Kyle A Jablonski, Jesus Arcos, Lucia Rosas, Tracey L Papenfuss, Jordi B Torrelles, Wael N Jarjour, and Mireia Guerau-de Arellano. CD38 Is Robustly Induced in Human Macrophages and Monocytes in Inflammatory Conditions. *Frontiers in immunology*, 9:1593, jul 2018.
- [33] Daphne Y.S. Vogel, Judith E. Glim, Andrea W.D. Stavenuiter, Marjolein Breur, Priscilla Heijnen, Sandra Amor, Christine D. Dijkstra, and Robert H.J. Beelen. Human macrophage polarization in vitro: Maturation and activation methods compared. *Immunobiology*, 219(9):695–703, 2014.
- [34] C A Ambarus, S Krausz, M van Eijk, J Hamann, T R D J Radstake, K A Reedquist, P P Tak,

BIBLIOGRAPHY

- and D L P Baeten. Systematic validation of specific phenotypic markers for in vitro polarized human macrophages. *Journal of immunological methods*, 375(1-2):196–206, 2012.
- [35] Rabia Bilge Özgül Özdemir, Alper Tunga Özdemir, Ayla Eker Sarıboyacı, Onur Uysal, Mehmet İbrahim Tuğlu, and Cengiz Kırmaz. The investigation of immunomodulatory effects of adipose tissue mesenchymal stem cell educated macrophages on the CD4 T cells. *Immunobiology*, 224(4):585–594, jul 2019.
- [36] Jeffrey A Barminko, Nir I Nativ, Rene Schloss, and Martin L Yarmush. Fractional factorial design to investigate stromal cell regulation of macrophage plasticity. *Biotechnology and Bioengineering*, 111(11):2239–2251, nov 2014.
- [37] Yuzo Kawata, Atsunori Tsuchiya, Satoshi Seino, Yusuke Watanabe, Yuichi Kojima, Shunzo Ikarashi, Kentaro Tominaga, Junji Yokoyama, Satoshi Yamagiwa, and Shuji Terai. Early injection of human adipose tissue-derived mesenchymal stem cell after inflammation ameliorates dextran sulfate sodium-induced colitis in mice through the induction of M2 macrophages and regulatory T cells. *Cell and Tissue Research*, 376(2):257–271, 2019.
- [38] European Medicines Agency. Search of Mesenchymal Stem Cells. https://www.ema.europa.eu/en/documents/assessment-report/alofisel-epar-public-assessment-report_en.pdf Accessed from:European Medicines Agency (EMA, 2021).
- [39] Peter J Murray, Judith E Allen, Subhra K Biswas, Edward A Fisher, Derek W Gilroy, Sergij Goerdt, Siamon Gordon, John A Hamilton, Lionel B Ivashkiv, Toby Lawrence, Massimo Locati, Alberto Mantovani, Fernando O Martinez, Jean-Louis Mege, David M Mosser, Gioacchino Natoli, Jeroen P Saeij, Joachim L Schultze, Kari Ann Shirey, Antonio Sica, Jill Suttles, Irina Udalova, Jo A van Genderachter, Stefanie N Vogel, and Thomas A Wynn. Macrophage activation and polarization: nomenclature and experimental guidelines. *Immunity*, 41(1):14–20, jul 2014.
- [40] Laura Chiossone, Romana Conte, Grazia Maria Spaggiari, Martina Serra, Cristina Romei, Francesca Bellora, Flavio Becchetti, Antonio Andaloro, Lorenzo Moretta, and Cristina Bottino.

BIBLIOGRAPHY

- Mesenchymal Stromal Cells Induce Peculiar Alternatively Activated Macrophages Capable of Dampening Both Innate and Adaptive Immune Responses. *Stem Cells*, 34(7):1909–1921, 2016.
- [41] Mario Roederer. Interpretation of cellular proliferation data: Avoid the panglossian. *Cytometry Part A*, 79 A(2):95–101, 2011.
- [42] Françoise Chapuis, Michelle Rosenzweig, Micael Yagello, Marianne Ekman, Peter Biberfeld, and Jean Claude Gluckman. Differentiation of human dendritic cells from monocytes in vitro. *European Journal of Immunology*, 27(2):431–441, feb 1997.
- [43] Lisa B Boyette, Camila Macedo, Kevin Hadi, Beth D Elinoff, John T Walters, Bala Ramaswami, Geetha Chalasani, Juan M Taboas, Fadi G Lakkis, and Diana M Metes. Phenotype, function, and differentiation potential of human monocyte subsets. *PLoS one*, 12(4):e0176460–e0176460, apr 2017.
- [44] Tanja Buchacher, Anna Ohradanova-Repic, Hannes Stockinger, Michael B Fischer, and Viktoria Weber. M2 Polarization of Human Macrophages Favors Survival of the Intracellular Pathogen *Chlamydia pneumoniae*. *PLoS one*, 10(11):e0143593–e0143593, nov 2015.
- [45] Angeles Domínguez-Soto, Elena Sierra-Filardi, Amaya Puig-Kröger, Blanca Pérez-Maceda, Fernando Gómez-Aguado, María Teresa Corcuera, Paloma Sánchez-Mateos, and Angel L Corbí. Dendritic Cell-Specific ICAM-3–Grabbing Nonintegrin Expression on M2-Polarized and Tumor-Associated Macrophages Is Macrophage-CSF Dependent and Enhanced by Tumor-Derived IL-6 and IL-10. *The Journal of Immunology*, 186(4):2192 LP – 2200, feb 2011.
- [46] Frank A W Verreck, Tjitske de Boer, Dennis M L Langenberg, Marieke A Hoeve, Matthijs Kramer, Elena Vaisberg, Robert Kastelein, Arend Kolk, René de Waal-Malefyt, and Tom H M Ottenhoff. Human IL-23-producing type 1 macrophages promote but IL-10-producing type 2 macrophages subvert immunity to (myco)bacteria. *Proceedings of the National Academy of Sciences of the United States of America*, 101(13):4560–4565, mar 2004.
- [47] Yong C. Lu, Wen C. Yeh, and Pamela S. Ohashi. LPS/TLR4 signal transduction pathway. *Cytokine*, 42(2):145–151, 2008.

BIBLIOGRAPHY

- [48] Siamon Gordon and Fernando O Martinez. Alternative activation of macrophages: mechanism and functions. *Immunity*, 32(5):593–604, 2010.
- [49] Maitane Ortiz-Virumbrales, Ramón Menta, Laura M Pérez, Ornella Lucchesi, Pablo Mancheño-Corvo, Álvaro Avivar-Valderas, Itziar Palacios, Angel Herrero-Mendez, Wilfried Dalemans, Olga de la Rosa, and Eleuterio Lombardo. Human adipose mesenchymal stem cells modulate myeloid cells toward an anti-inflammatory and reparative phenotype: role of IL-6 and PGE2. *Stem Cell Research & Therapy*, 11(1):462, 2020.
- [50] Michael R Elliott, Kyle M Koster, and Patrick S Murphy. Efferocytosis Signaling in the Regulation of Macrophage Inflammatory Responses. *Journal of immunology (Baltimore, Md. : 1950)*, 198(4):1387–1394, feb 2017.
- [51] C L Holness and D L Simmons. Molecular cloning of CD68, a human macrophage marker related to lysosomal glycoproteins. *Blood*, 81(6):1607–1613, 1993.
- [52] Gilberto R Sambrano and Daniel Steinberg. Recognition of oxidatively damaged and apoptotic cells by an oxidized low density lipoprotein receptor on mouse peritoneal macrophages: role of membrane phosphatidylserine. *Proceedings of the National Academy of Sciences of the United States of America*, 92(5):1396–1400, 1995.
- [53] M P Ramprasad, W Fischer, J L Witztum, G R Sambrano, O Quehenberger, and D Steinberg. The 94- to 97-kDa mouse macrophage membrane protein that recognizes oxidized low density lipoprotein and phosphatidylserine-rich liposomes is identical to macrosialin, the mouse homologue of human CD68. *Proceedings of the National Academy of Sciences of the United States of America*, 92(21):9580–9584, 1995.
- [54] Mallery C Greenlee-Wacker. Clearance of apoptotic neutrophils and resolution of inflammation. *Immunological reviews*, 273(1):357–370, 2016.
- [55] Valerie A Fadok, Donna L Bratton, S Courtney Frasch, Mary L Warner, and Peter M Henson. The role of phosphatidylserine in recognition of apoptotic cells by phagocytes. *Cell Death & Differentiation*, 5(7):551–562, 1998.

BIBLIOGRAPHY

- [56] Elizabeth Mendoza-Coronel and Enrique Ortega. Macrophage Polarization Modulates Fc γ R- and CD13-Mediated Phagocytosis and Reactive Oxygen Species Production, Independently of Receptor Membrane Expression. *Frontiers in immunology*, 8:303, mar 2017.
- [57] Therese Liechtenstein, Ines Dufait, Alessio Lanna, Karine Breckpot, and David Escors. MODULATING CO-STIMULATION DURING ANTIGEN PRESENTATION TO ENHANCE CANCER IMMUNOTHERAPY. *Immunology, endocrine & metabolic agents in medicinal chemistry*, 12(3):224–235, sep 2012.

5 Appendix

5.1 Monocytes

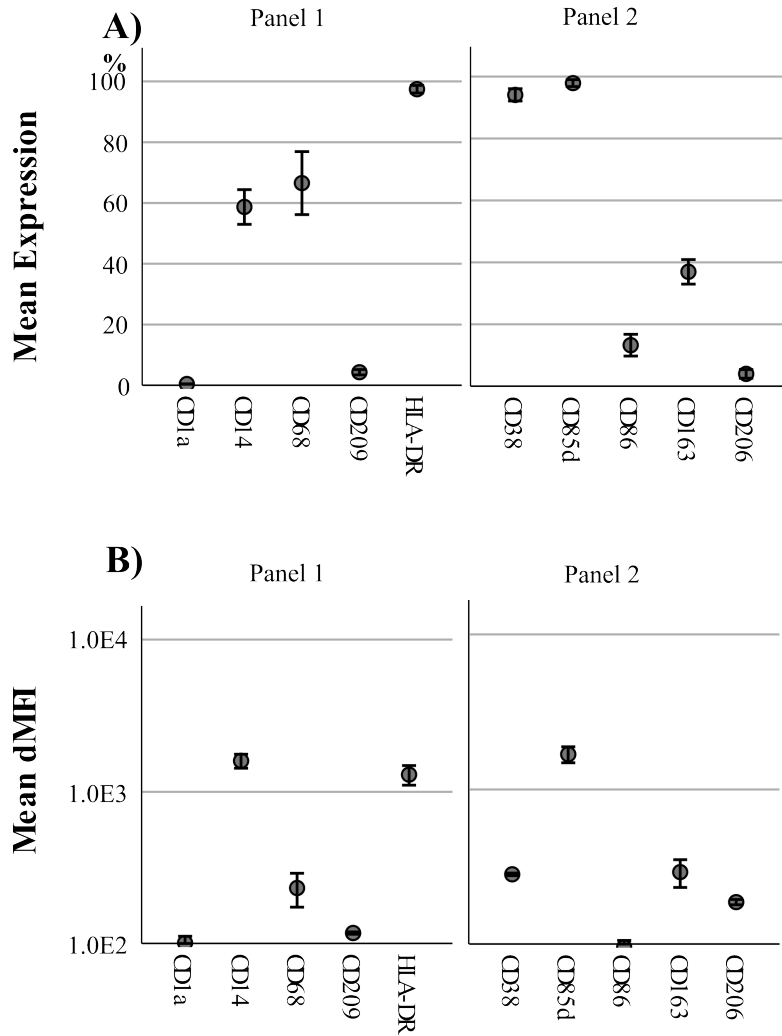


Figure 5.1: A) the percentage of monocytes expressing a surface marker of Panel 1 or Panel 2. B) dMFI for each surface marker. n=4

5.2 Activation of M1 macrophages

Instead of washing the wells with detached cells in MACS buffer, the cells were collected and the wells were washed with PBS, as described in section 2.4. To further investigate the toxicity and the adjusted method, immature macrophages were either activated with 100 ng/ml LPS or 500 ng/ml LPS in combination with the different concentration of IFN- γ . The viability of the cells increases significantly, illustrated in figure 5.2.

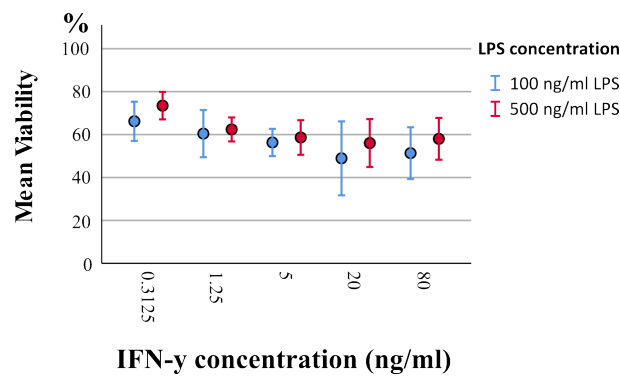


Figure 5.2: Viability of M1 macrophages with 100 or 500 ng/ml LPS in combination with different concentration of IFN- γ

5.3 Activation of M2c macrophages

M2c IL-10 secretion

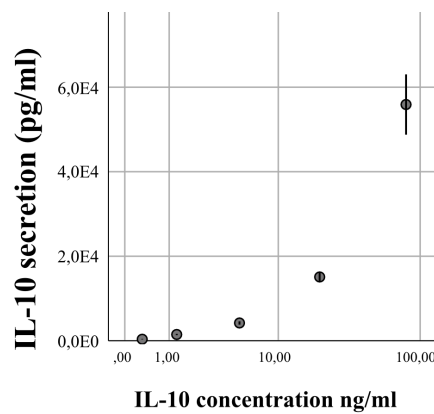


Figure 5.3: Mean secretion of IL-10 secreted by M2c macrophages, activated with different concentration of IL-10

5.4 Dendritic Cells

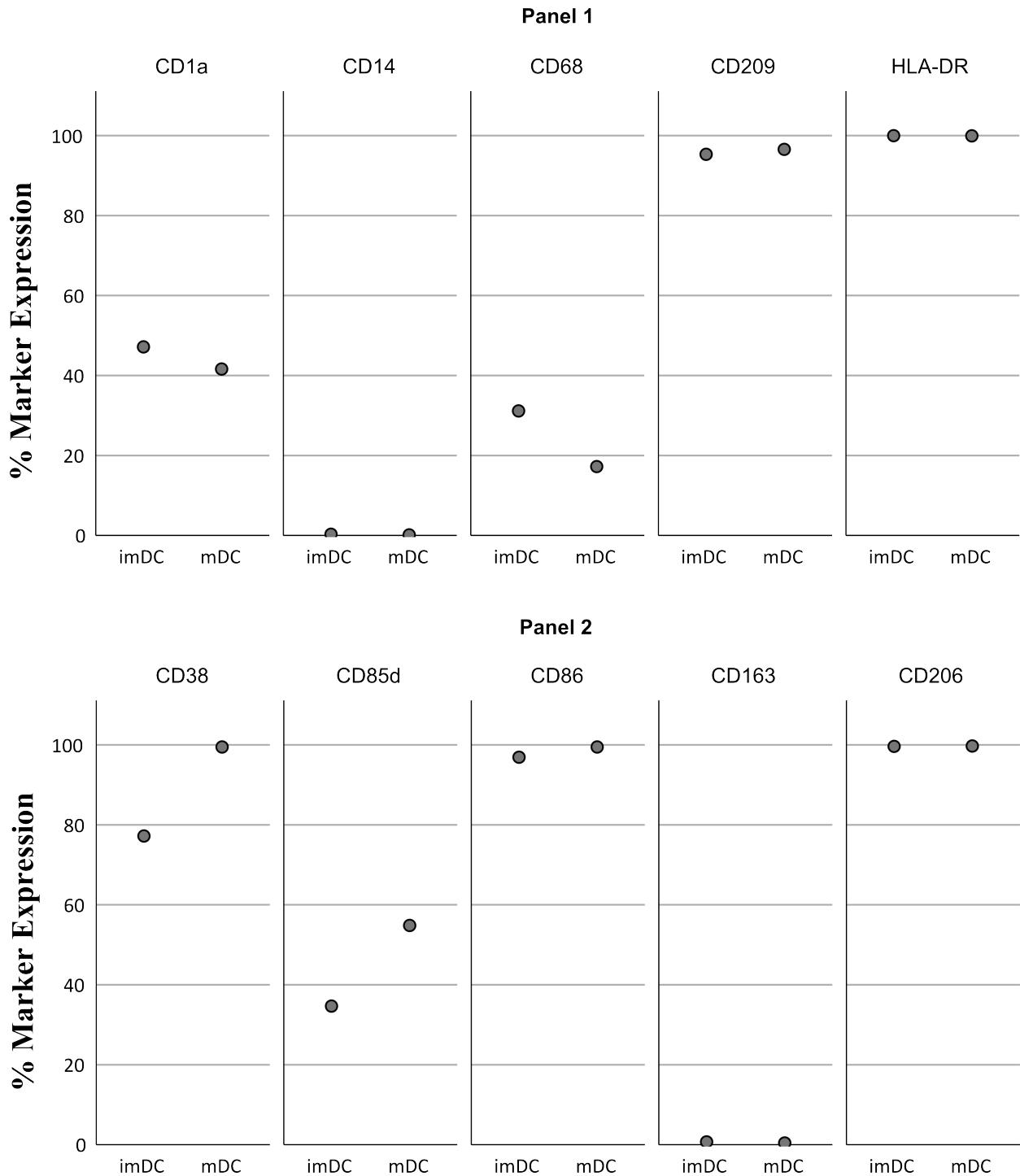


Figure 5.4: Representative marker expression of immature and mature Dendritic Cells (imDC) and (mDC) from a single donor. Data kindly provided by Camilla Holm Pedersen